DESIGN AND DOSIMETRY CONSIDERATION FOR THE FABRICATION OF MANUAL MULTILEAF COLLIMATOR FOR A CIRUS COBALT-60 TELETHERAPY MACHINE

A THESIS SUBMITTED TO THE

DEPARTMENT OF MEDICAL PHYSICS

SCHOOL OF NUCLEAR AND ALLIED SCIENCES

UNIVERSITY OF GHANA

BY

SAVANNA NYARKO

(10443885)

BSc, UNIVERSITY OF CAPE COAST, 2012

IN PARTIAL FULFILMENT OF THE REQUIREMENTS FOR

THE AWARD OF A

MASTER OF PHILOSOPHY DEGREE IN MEDICAL PHYSICS

JULY, 2015

DECLARATION

This thesis is the result of research work undertaken by SAVANNA NYARKO in the Department of Medical Physics, School of Nuclear and Allied Sciences, University of Ghana, under the supervision of Prof. Cyril Schandorf, Prof. A.W.K. Kyere and Mr. Eric K.T. Addison.

…… Date …….

SAVANNA NYARKO

(STUDENT)

…… Date …….

Prof. Cyril Schandorf

(PRINCIPAL SUPERVISOR)

…… Date …….

Prof. A.W.K. Kyere

(CO-SUPERVISOR)

…… Date ……

Mr. Eric K.T. Addison

(CO-SUPERVISOR)

ABSTRACT

A manual eight multi-leaf collimator (MLC) has been designed and fabricated for the Cirus cobalt-60 machine at the Komfo Anokye Teaching Hospital. The fabricated MLC is made up of a high carbon steel leaves. The leaf in each bank has a standard width of 7.5 cm projected at the isocentre at a thickness of 4.6 cm. The leaf transmission factor was determined to be 4.8%, which is within the acceptable standard of below 5%. The cobalt-60 beam characteristics such as beam profiles, output factors, MLC effect were determined. Inter-leaf leakage was determined with the 2D dose profile showing a linear increase between field size and leakage at the ends of the leaves. Output factors measurements were done for open and closed fields using an ion chamber and a 30 x 30 cm^2 water phantom. The MLC output factor was measured for square fields from 4 x 4 to 32 x 32 cm^2 and varying the depths from 0.5 to 15 cm in steps of 0.5cm. Output factors for open MLC fields ranged from 0.952 to 1.250. The MLC effects were measured for square and rectangular fields and depth dependent within the phantom. MLC effect measurement for 7.5 and 15 cm square fields had output factor ranges of 0.979 to 1.218 and 1.143 to 1.218 respectively. The fabricated MLC needs further refinement in terms of the number of leaves, design of the ends of the leaves and limiting the interleaf leakage radiation.

DEDICATION

This work is dedicated to my dear parents Nana Kobina Amoansah and Madam Sarah Sam, my entire family and my future husband.

ACKNOWLEDGEMENTS

I wish to express my profound gratitude to the ALMIGHTY GOD for His Abundant Grace, Mercies, Strength, Love, Goodness, Kindness and Uncommon Favour upon my life.

My sincere appreciation goes to my supervisors, Prof. Cyril Schandorf, and Prof. A.W.K. Kyere, the Head of the Department of Medical Physics, for their valuable contributions, guidance, patience, encouragement and suggestions in the preparation of this thesis.

I would sincerely give thanks to Mr Eric K.T. Addison, the Head of medical physics unit of the Komfo Anokye Teaching Hospital (KATH), Oncology Directorate, for his huge guidance and supervision, encouragements and for his immense support and work toward the experimental methods set for this thesis work. Furthermore, I would like to thank Mr Aziz Abdul, Mr Alex Kwame Appiah and Mr Yaw Brefo, all of Suame Magazine for helping me acquire the fabrication of the multi-leaf collimator. I also thank Mr Ernest Eduful of Ghana Atomic Energy Commission (GAEC), Linus Owusu Agyapong, Samuel Odame Obeng and Kofi Sarpong for your wonderful contribution towards the success of this thesis. To you all I say, GOD BLESS YOU.

Finally, generally I am grateful to the Oncology Directorate, KATH and in particular to the medical physics staff members, radiation therapists, oncologists and the national service persons of 2014/2015 for their immense collaboration and guidance in my daily activity in the hospital where they have played a major role in my practical work and experimental data collection if it was not because of them this project thesis work might not have been possible.

TABLE OF CONTENTS

LIST OF PLATES

LIST OF ABBREVIATIONS

AAPM	American Association of Physics in Medicine
BEV	Beam's Eye View
CF	Collimator factor
CRT	Conformal Radiation Therapy
Co-60	Cobalt-60 source
CT	Computed tomography
DCP	Dose to small mass of medium
Do	Reference depth
HVL	Half value layer
IAEA	International Atomic Energy Agency
ICRP	International Commission on Radiological Protection
ICRU	International Commission on Radiation Units/ Measurements
IGRT	Image Guided Radiation Therapy
IMRT	Intensity Modulated Radiation Therapy
MLC	Multi-leaf Collimator
NTCP	Normal Tissue Complication Probability

OF	Output factor
PDD	Percentage Depth Dose
PMMA	Polymethyl methacrylate
PSF	Peak Scatter Factor
PTV	Planning Target Volume
QA	Quality Assurance
QC	Quality Control
SAD	Source to Axis Distance
Sc	Collimator Scatter Factor
SCP	Total Scatter Factor
Sp	Phantom Scatter factor
SSD	Source to Surface Distance
TCP	Tumour Control Probability
TF	Transmission Factor
VMAT	Volumetric Arc Therapy
WF	Wedge factor
X	Collimator Width (lower jaw)
Y	Collimator Length (upper jaw)

LIST OF SYMBOLS

A	Field size
Bs	Ambient pressure
Ci	Curie
cm	Centimetre
D^*	Physical dose quantity
D	Absorbed dose
E	Energy
Gy	Gray
hν	Energy
K	Mean of readings
KW	Kilowatt
M	Mass
M_w	Mean check source measurements
Mg/kg	Milligram per kilogram
MV	MegaVoltage
nC	Nano coulomb
$N_{D,W}$	Estimated uncertainty reference value

P	Measured average atmospheric pressure
P	Dose at a point
q	Amount of charge
$\mathbf{Q_{measured}}$	Measured check source value
Q	Quantity
R.H.	Relative humidity
T	Measured average temperature
V	Voltage
Z	Atomic number of an element
z	depth
ɣ	Gamma ray
$^{o}\mathbf{C}$	Degree Celcius
$_{5}\mathbf{D_w}$	Absorbed dose to water rate
µ	Attenuation coefficient

CHAPTER ONE

INTRODUCTION

1.1 BACKGROUND

Radiation was first used therapeutically in the late 1800s. Radiation therapy treatment machines have evolved from very low energy x-ray machines into a variety of treatment options that include high-energy electrons, high-energy photons, and even heavier particles such as neutrons or protons. The goal of radiation therapy is to kill tumour cells while at the same time limiting the dose to normal tissues. Large doses of radiation to healthy tissues will not only make the patient more uncomfortable through the course of treatment but can also leave lasting complications, depending upon the type of tissue that is irradiated and the dose the healthy tissue receives (Ferachi, 2003).

Shaping the beam is an important way of minimizing the absorbed dose in healthy tissue and `critical structures (Jeraj and Robar, 2004). Radiation is conformed to the tumour volume in several different ways. The most straightforward method is blocking non-involved areas from the radiation beam (Ferachi, 2003). This can be achieved by using multi-leaf collimators or custom (conventional) blocks. Conventional blocks consist of either a set of lead blocks having a range of shapes and sizes that are placed by hand at each treatment session or cerrobend blocks fabricated individually for a given field applied to a specific patient (Power et al., 1973). The beam passes through these lead-alloy shields which block portions of the rectangular radiation field outside the target volume. The beam blocks are fabricated based on the patient's treatment plan, using radiographic plane films or CT scan data.

A single patient may have as many as 10 radiation fields used during treatment, each with a different shape and requiring unique beam block (Boyer et al., 2001). Conformal radiotherapy is a modern technique in which each field is shaped to conform to the shape of the tumour volume by using multi-leaf collimator (MLC).

The multileaf collimator is an important new tool for radiation therapy dose delivery (Galvin, 1993). A MLC is made up of many opposed pairs of small leaves mounted into two carriages on either side of the field (Ferachi, 2003). The advantages of MLCs are; simple and less time consuming preparation, use without the need to enter the treatment room and simple change or correction of field shape. The therapy expenses are lower because individual shielding blocks are not needed, thus eliminating the need to handle the Wood's alloy, which is toxic. With MLC, the therapy time is shortened (Jeraj and Robar, 2004).

The various types of MLCs that are currently available commercially have different leaf widths and number of leaves. Originally, they had been introduced as a substitute for alloy block field shaping but, they are used for intensity modulated radiotherapy as well (Topolnjak, 2004). Intensity modulated radiation therapy (IMRT) is a revolutionary type of external beam treatment that is able to conform radiation to the size, shape and location of a tumour (Goadrich, 2004).

1.2 STATEMENT OF THE PROBLEM

Basic goal of radiotherapy treatment is the irradiation of a target volume while minimizing the amount of radiation absorbed in healthy tissue. Shaping the beam is an

important way of minimizing the absorbed dose in healthy tissue and critical structures.

Since the inception of Komfo Anokye Teaching Hospital Radiotherapy Centre about ten (10) years ago, there has been the use of fabrication of conventional or customized blocks for conforming radiation fields to a target shape. Manufacturing of the conventional or customized block is labour intensive and they are cumbersome to use because of their weight. It can fall on the patient if it is not mounted or positioned well and can also injure the therapist whiles standing in an awkward position.

This study is therefore being undertaken to design and fabricate a manual multi-leaf collimator for clinical applications at the Komfo Anokye Teaching Hospital Radiotherapy Centre to improve the efficiency of treatment delivery.

1.3 OBJECTIVES OF THE RESEARCH

The principal objective of this research is to fabricate a manual multi-leaf collimator (MLC) for clinical applications at the Komfo Anokye Radiotherapy Centre.

The specific objectives of this research work are:

Using these constructed MLCs in radiation oncology to improve the efficiency of treatment delivery.

i) The basic dosimetric parameters (output factors, beam profile and MLC effect) will be measured and compared with the international data.

ii) Make appropriate recommendations from the findings for the improvement of treatment delivery to patients.

1.4 RELEVANCE OF RESEARCH

It is now recognized that safe and effective radiotherapy service needs not only substantial capital investment in radiotherapy equipment and specially designed facilities but also continuous investment in maintenance and upgrading of the equipment.

The findings of this research work will assist medical physicists, radiation therapists, and radiation oncologists with the acquisition, testing, commissioning, daily use, and quality assurance (QA) of MLCs in order to realize increased efficiency of utilization of therapy facilities.

MLC will replace conventional or customized blocking, thereby eliminating the effort and cost of fabricating customized blocks, the need for storage space for blocks and other practical difficulties during the process of the block making. Conformal therapy will continuously adjust the field shape to match the beam's eye view (BEV) projection of a planning target volume (PTV). It will help the Centre develop confidence in the radiation treatment they offer to patients by optimizing the tumour control probability (TCP) whilst minimizing the normal tissue complication probability (NTCP). It will help in minimizing the probability of accidents occurring. The outcome of this research work would be used to achieve beam-intensity modulation, which is an advanced form of conformal therapy.

1.5 SCOPE AND DELIMITATION

This research will be performed at the Komfo Anokye Teaching Hospital Radiotherapy Centre.

In this research work, PTW 2D array detector will be used to obtain the basic dosimetric parameters such as, leaf transmission, output factors, dose profiles and MLC effect of the fabricated multi-leaf collimator (MLC).

1.6 ORGANIZATION OF THESIS

The thesis is organized as follows: The first chapter deals with the introduction of the concept of study, second chapter deals with the literature review on the subject of study, third chapter is about the materials and methods used to solve the problem stated in the first chapter. The fourth chapter gives the results obtained and discussions in terms of the validity and implications on the expected outcome of the research study in relation to the published data sources. In chapter five of the thesis, conclusions and recommendations are made.

CHAPTER TWO

LITERATURE REVIEW

2.1 INTRODUCTION

X-rays were discovered on 8th December 1895 by Wilhelm Rontgen in Germany. X-rays carry a high amount of energy, which has the ability to ionize atoms and make their bonds unstable. This makes it highly harmful to living cells. An overdose or under dose of exposure can cause radiation induced cancer. At the same time, ionizing radiation can be used to kill malignant cells in radiation therapy. In January 1896, an intern medical student used x-rays to treat a cancer patient called Rose Lee of breast cancer successfully, after the recommendations of Leopold Freund and Eduard Schiff (Topolnjak, 2005).

In early 1990, MLC was introduced into radiation therapy to replace the manual beam shaping blocks for used in linear accelerators. It has since become the accepted standard for linear accelerators.

2.2 FIELD SHAPING

Field shaping technique has been widely implemented to upgrade conventional radiotherapy to a three-dimensional conformal radiation treatment. The benefits of dose conformity to the target volume while sparing dose to normal tissues and improving target dose uniformity have been discussed in several publications. The technique is based on adjusting the beam initially with a few conformal static beams through the use of a number of custom blocks made of lead alloy. With the development of the multi-leaf collimator (MLC), the field shape can be dynamically conformed to the target during gantry rotation (Wong, 2004).

External photon beam radiotherapy is usually carried out with more than one radiation beam in order to achieve a uniform dose distribution inside the target volume and as low as possible a dose in healthy tissues surrounding the target. ICRU Report No. 50 recommends a target dose uniformity within +7% and –5% of the dose delivered to a well-defined prescription point within the target (ICRU 50.1993, Parker and Patrocinio, 2005).

Once the collimators have been opened to the desired field size that encompasses the tumour, the physician may decide to block out some normal tissue that remains in the treatment field. This is accomplished by placing blocks (or alloy), constructed of a combination of bismuth, tin, cadmium, and lead, in the path of the beam. In this way, normal tissues are shielded and the dose can be delivered to the tumour at a higher level than if the normal structures were in the field. These individually constructed blocks are used in both x-ray and electron treatments. A more modern technique involves multi-leaf collimators mounted inside the gantry (Gadza et al., 2004).

Shielding of vital organs within a radiation field is one of the major concerns of radiation therapy. Considerable time and effort are spent in shaping fields not only to protect critical organs but also to avoid unnecessary irradiation of the surrounding normal tissue.

Attendant to this problem is its effect on skin dose and the build-up of dose in the subcutaneous tissue. Skin sparing is an important property of megavoltage photon beams, and every effort should be directed to maintaining this effect when irradiating normal skin (Khan, 2003).

Multileaf collimators (MLC) for conforming radiation fields to a target's shape have been in use for more than 20 years (Baumann et al., 2012).The use of MLC field shaping is likely to save time and to incur a lower operating cost when compared to the use of beam blocks; fabrication facilities and expenses will be reduced. Patient setup time during treatment may also decrease, allowing greater patient throughput (Boyer et al., 2001).

2.3 BEAM MODIFICATION IN RADIOTHERAPY

Radiation reaching any point is made up of primary and scattered photons. Any introduction of the modification devices results in alteration of dose distribution.

Beam modification is defined as desirable modification in the spatial distribution of radiation within the patient by insertion of any material in the beam path (Sharma, 2012).

2.3.1 TYPES OF BEAM MODIFICATION

Shaping of the radiation beam before it reaches the patient is accomplished using several devices (Ferachi, 2003). A method for making a beam modifier to be used in radiation therapy includes defining a region of interest in the patient that is to receive radiation, with the region of interest being defined using an anatomic coordinate system format. There are four types of beam modifiers (Sharma, 2012):

(i) Shielding

To eliminate radiation dose to some special parts of the zone at which the beam is directed.

(ii) Compensation

To allow normal dose distribution data to be applied to the treated zone, when the beam enters an or obliquely through the body or where different types of tissues are present.

(ii)Wedge Filtration

Where there is a special tilt in isodose curves at the central ray of a beam at a specified depth (Dumitru et al., 2012).

(iv) Flattening

Where the spatial distribution of the natural beam is altered by reducing the central exposure rate relative to the peripheral.

2.4 DOSIMETRY

Radiation dosimetry is a process whereby a signal is recorded through interactions of the incident radiation with matter causing a measurable change in its properties. This can be a change in the measured charge (ionization chambers), measured light output (TLD) or a visible polymeric chemical reaction (radiochromic film). The process is caused by atomic and nuclear interactions occurring within the atom (Buston et al., 2003).

Dosimetry is the measurement of the absorbed dose delivered by ionizing radiation, the term is better known as a scientific sub-specialty in the fields of health physics and medical physics, where it is the calculation and assessment of the radiation dose received by the human body.

2.4.1 DOSIMETRIC CHARACTERISTICS OF MULTI-LEAF COLLIMATOR (MLC)

The three-dimensional conformal radiotherapy (3D-CRT), intensity-modulated radiotherapy (IMRT), and image-guided radiotherapy (IGRT) are the most advanced techniques in radiotherapy, which use irregular fields–using multileaf collimators. The accuracy of these techniques depends on dosimetric characteristics of the multi-leaf collimators (Kotb et al., 2013).

The dosimetric characteristics include leaf transmission, output factors, percentage depth doses, electron contamination and penumbra.

2.4.2 DOSIMETRIC PARAMETERS

During dosimetric processes, three paramount parameters stand out and are the basics for all dosimetric work.

2.4.2.1 Depth

The larger is the field size, the deeper is the depth of the peak and the larger is the scatter function. The larger the depth in phantom, the smaller is the relative primary component and the larger is the relative scatter component.

2.4.2.2 Distance

This takes into accounts two factors. The source-skin distance and the source-collimator distance. The distance and shielding between the patient or the worker and the source of radiation is very important.

2.4.2.3 Field size (scatter)

This is defined on a patient's surface. It is the equivalent square of the field size incident on the phantom. The field size is reduced by the MLCs. The field size e.g. A is defined at point Q, which is normally placed into the isocenter of the treatment machine.

Radiation fields are divided into two categories: geometric and dosimetric (physical) field sizes. According to the ICRU, the geometric field size is defined as "the projection of the distal end of the machine collimator onto a plane perpendicular to the central axis of the radiation beam as seen from the front center of the source." Figure 2.1 shows the SAD setup with field size.

The dosimetric field size (also called the physical field size) is defined by the intercept of a given isodose surface (usually 50% but can also be up to 80%) with a plane perpendicular to the central axis of the radiation beam at a defined distance from the skin. Zero area fields are a hypothetical radiation fields in which the dose at depth z in phantom is entirely due to primary photons, since the volume that can scatter radiation is zero.

As the field size increases, PSF first increases from unity linearly as field size increases and then saturates at very large fields. The beam quality at which the maximum back scatter occurs shifts toward harder radiation with an increase in field size. It also considers equivalent square or rectangular field and equivalent circle for square fields. Using Days' rule for the arbitrary rectangular field with sides X and Y,

$$\frac{XY}{2(X+Y)} = \frac{X_{EQ}^2}{4X_{EQ}} \qquad \mathbf{2.1}$$

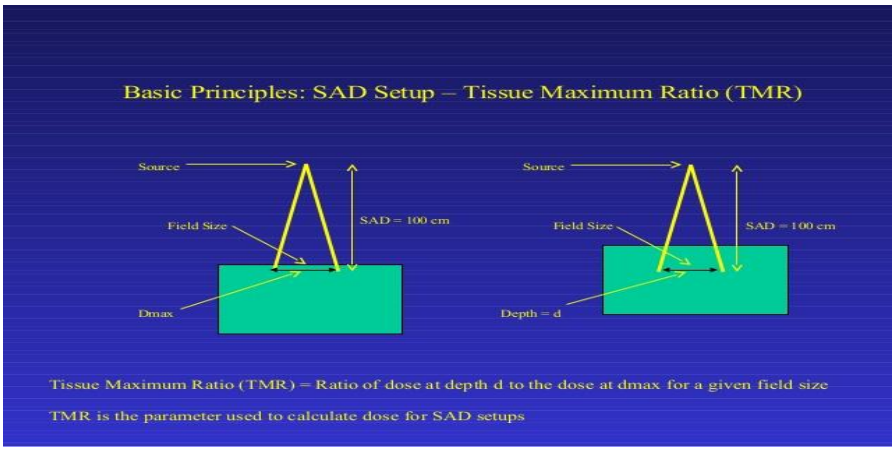

Plate 2.1 SAD set up with field size

2.4.3 COMPARISON OF VARIOUS MULTILEAF COLLIMATORS

Shaping of the radiation beam before it reaches the patient is accomplished using several devices. The first of these is the secondary collimators. These collimators consist of jaws that are under motor control and can be moved to create a rectangular field of any size up to 40 cm by 40 cm at isocenter. The secondary collimator jaws move along an arched path to follow beam divergence and shape the beam in two dimensions.

Secondary collimators are used to shape a rectangular field, but because no tumour volume is rectangular in shape, additional methods are needed to further contour the beam to the tumor volume. Additional field shaping can be done in either two or three dimensions with a tertiary collimator. Traditional tertiary blocking or beam shaping is most commonly accomplished by custom-made cerrobend blocks. Another tertiary collimator that almost completely eliminates the need for custom blocks and therefore reduces production time is the multileaf collimator (MLC). A MLC is made up of many opposed pairs of small leaves mounted into two carriages on either side of the field. The leaves may be extended under motor control to shape a field that is conformal to the tumour volume. The location of the MLC on the accelerator head depends upon the accelerator manufacturer (Ferachi, 2003).

MLCs produced by various manufacturers employ special mechanisms to move the leaves accurately to their prescribed positions (Jeraj and Robar, 2004). The various types of MLCs that are currently available commercially have different leaf widths and number of leaves (Topolnjak, 2005).

2.4.3.1 Varian System

For each Varian MLC, two banks of independent tungsten alloy leaves face each other and travel linearly perpendicular to the beam central axis. Orthogonal to the direction of motion, the leaf edge is parallel to the beam ray line from the target (Hariri and Shahriari, 2010).

Varian produces an MLC with 60 leaf pairs and a field size of 40 x 40 cm^2. In the central 20 cm of the field the leaf width is 0.5 mm while in the outer 10 cm on both sides of the field the leaf width is 1 cm. With such a design a high resolution is achieved in the central part of the field, but unfortunately not in the outer part (Topolnjak, 2004).

The Varian MLC is positioned as a tertiary system below the standard adjustable jaws. This design was used for two major reasons: first, the approach facilitates the retrofitting of the MLC onto existing units, second, the designers of this system felt that any failure of the system should not be allowed to take the entire accelerator out of service, and provisions were made to manually move offending leaves (Galvin, 1993b).

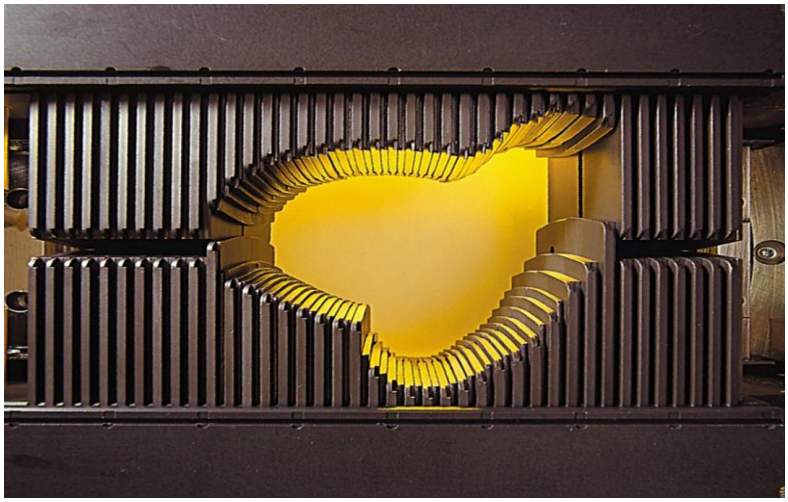

Plate 2.2 Varian multi-leaf collimator

2.4.3.2 Elekta System

In the Elekta design, the MLC leaves move in the y-direction (parallel to the axis of rotation of the gantry) (AAPM Report no. 72; TG 50, 2006).

The upper jaw is replaced by the MLC leaves and a back-up diaphragm placed beneath the leaves follows the leave to provide additional attenuation (AAPM Report no. 72, 2006).

Plate 2.3Elekta multi- leaf collimator

2.4.3.3 Siemens System

Siemens has MLCs with straight tip and double focus leaves (Das et al., 1998; Topolnjak, 2005). Siemens has chosen to mount their MLC as a replacement for the lower standard jaw system. This geometry gives an intermediate leaf width dimensions, relative to the other two manufacturers, for the same projected size at isocenter. This positioning creates a favourable geometry for the use of arcing trajectories so that the leading edge of each leaf follows beam divergence (Galvin, 1993b).

Plate 2.4 Siemens multi-leaf collimator

2.5. DOSIMETRY MEASUREMENTS FOR MULTI LEAF COLLIMATOR

2.5.1 Reference checks source measurements.

The output of an ionisation chamber is dependent on the ambient conditions (temperature, pressure and relative humidity), age (date of calibration) and level of usage. This protocol measurement is to establish the constancy of the chamber using a long – lived radionuclide source.

Corrected measured ionisation readings in coulombs are always compared with previous reading for leakage and drift. The corrected reading is given in equation 2.2

$$\boldsymbol{f Q_{Corr.Reading} = Q_{measured} \times k(T,P)} \qquad \textbf{2.2}$$

Where $Q_{Corr.\ Reading}$ = Corrected Ionisation Reading in Coulombs (nC/time)

T= measured average temperature (^oC)

P= measured average atmospheric pressure (KPa)

$Q_{measured}$ = measured check source value (nC/time)

2.5.2 Absorbed dose measurements

Technical Report Series 398 was used for determination of absorbed dose in a patient irradiated by beams of X or gamma rays in radiotherapy procedures, the International Commission on Radiation Units and Measurements (ICRU) concluded that although it is too early to generalize, the available evidence for certain types of tumour, points to the need for an accuracy of ±5% in the delivery of an absorbed dose to a target volume if the eradication of the primary tumour is sought. The requirement for accuracy of 5% in the delivery of absorbed dose would correspond to a combined uncertainty of 2.5% at the level of one standard deviation. Today it is considered that a goal in dose delivery to the patient based on such an accuracy requirement is too strict and the figure should be increased to about one standard deviation of 5%, but there are no definite recommendations in this respect. The requirement for accuracy of ±5% could, on the other hand, also be interpreted as a tolerance of the deviation between the prescribed dose and the dose delivered to the target volume (TRS 398).

Absorbed dose to water is the quantity of main interest in radiation therapy, since this quantity relates closely to the biological effects of radiation.

The absorbed dose to water at the reference depth z_{ref} in water for a reference beam of quality Q_o and in the absence of the chamber is given by;

$$D_{w,Q_o} = M_{Q_o} N_{D,w,Q_o} \qquad \textbf{2.3}$$

where,

M_{Q_o} is the reading of the dosimeter under the reference conditions used in the standards laboratory (nC)

$N_{D,w,Qo}$ is the calibration factor in terms of absorbed dose to water of the dosimeter obtained from a standards laboratory.

The advantages of calibrations in terms of absorbed dose to water and dosimetry procedures using these calibration factors are;

1. Reduced uncertainty

The rationale for changing the basis of calibrations from air kerma to absorbed dose to water was the expectation that the calibration of ionization chambers in terms of absorbed dose to water would considerably reduce the uncertainty in determining the absorbed dose to water in radiotherapy beams. Measurements based on calibration in air in terms of air kerma require chamber dependent conversion factors to determine absorbed dose to water.

2. A more robust system of primary standards

Despite the fact that the quantity of interest in radiation dosimetry is absorbed dose to water, in the past years, most national, regional and international dosimetry recommendations are based on the use of an air kerma calibration factor for an ionization chamber, traceable to a national or international primary standard of air kerma for Co-60 gamma radiation. Although international comparisons of these standards have exhibited very good agreement, a substantial weakness prevails in that all such standards are based on ionization chambers and are therefore subject to common errors.

3. Use of a simple formalism

The formalism given in Equation 2.3 and in most national and international dosimetry protocols for the determination of absorbed dose to water in radiotherapy beams is based on the application of several coefficients, perturbation and other correction factors. This is because of the practical difficulty in making the conversion from the free-air quantity air kerma to the in-phantom quantity absorbed dose to water.

2.5.3 Percentage depth dose

This is a quotient expressed as a percentage of the absorbed dose at any depth to the absorbed dose at a fixed referenced depth (Do) along the central axis of beam. The percentage depth dose increases with increasing beam energy. Higher-energy beams have greater penetrating power and thus deliver a higher-percentage depth dose. When the effects of inverse square law and scattering are not considered, the percentage depth dose variation with depth is approximately the same as exponential attenuation. Therefore, the beam quality affects the percentage depth dose by virtue of the average attenuation coefficient μ. As the μ decreases, the more penetrating the beam becomes, resulting in a higher percentage depth dose at any given depth beyond the build-up region. (Khan, 2003).

For small fields it is assumed that the depth dose at a point is effectively the result of the primary radiation, that the photons have traversed the overlying medium without interacting. The contribution of the scattered photons to the depth dose in this case is either zero or negligible. As the field size is increased, the contribution of the scattered radiation to the absorbed dose increases. This is so because an increase in scattered dose is greater at larger depths than at the depth of Dmax. The percent depth

dose increases with increasing field size. This increase depends on beam quality. Since the scattering probability or cross section decreases with energy increase and the higher-energy photons are scattered more predominantly in the forward direction, the field size dependence of percent depth dose is less pronounced for the higher-energy than for the lower-energy beams. Percent depth dose increases with SSD because of the effects of the inverse square law (www.medicalphysics.org). Dose measurements are generally made in water or "water equivalent" plastic with an ionization chamber, since water is very similar to human tissue with regards to radiation scattering and absorption.

It is represented mathematically as;

$$Percentage\ Depth\ Dose = \frac{D_d}{D_o} \times 100 \qquad \textbf{2.4}$$

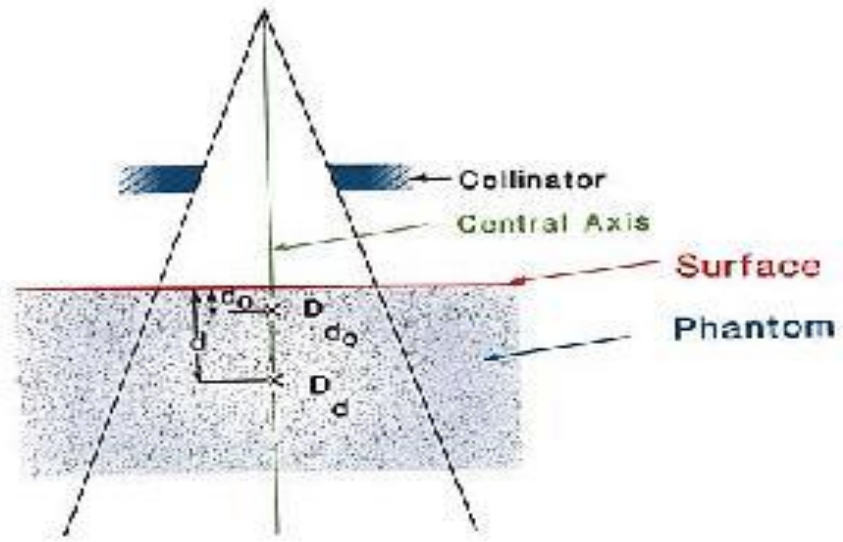

Plate 2.5 Setup measurement for P.D.D

2.5.4 Total scatter factor

This is a product of the collimator scatter factor and phantom scatter factors. Thus, a widely accepted practice is to measure dose and output factors at depths (5-10 cm). However, the validity of the definition of SCP must be maintained. Denoting SCP (A, d) as the total scatter factor measured at a depth d in a phantom for field size A, the values of SCP (A, dmax) can be calculated using the formula.

SCP= SP X SC or

$$SCP(A, D_{MAX}) = \frac{SCP(A,D)}{PDD(A,D)/PDD(10,D)} \qquad \textbf{2.5}$$

Where PDD (A, d) is the percent depth dose.

SCP (A, d) is the total scatter factor

This research would determine the SCP (A, d) at different depths in a water phantom over the range of field size (2-40 cm) for cobalt-60 beam.

2.5.5 Output factor.

Output of the CIRUS cobalt-60 machine is the dose determined by an ion chamber at reference field size that will produce 1cGy/time. Output factor as defined by F. M. Khan is also known as collimator scatter factor (Sc) which is the ratio of output in air for a given field to that for a 10 x 10 cm^2 field this is measured by an ion chamber. Khan does not identify any depth for the measurement of output. It is the ratio of output at D_{max} for a given field size to output at D_{max} for reference 10 cm x 10 cm. (AAPM 1999, IAEA 2004). Khan has called this as total scatter factor (Sc, p). It is mathematically represented as the product of collimator scatter factor and the phantom scatter factor

(OF = CF X SF) **2.6**

It can also be defined as the dose and any field size per dose at 10 x 10cm^2. OF > 1 if the field size is larger than 10x10cm^2

OF < 1 if the field size is smaller than 10x10 cm^2

For quality assurance OF is measured at Dmax and SSD 100 cm in a water phantom, collimator scatter factor (Sc) is measured in air at SAD 100 cm and Dmax, using buildup cap. Phantom scatter factor (Sp) is not measured practically but can be found by dividing OF by Sc (Sp=OF/Sc).

2.5.6 Beam profiles for open and wedge fields

Traditionally, there are four physical wedges (15°, 30°, 45° and 60°). It is commonly assumed that non-physical wedges do not alter the photon spectrum compared with physical wedges that introduce beam hardening and loss of dose uniformity in the unwedged direction.

Megavoltage beam profiles consist of three regions:

1. Central region represents the central portion of the profile extending from the central axis to within 1 cm to 1.5 cm of the geometric field edges of the beam.
2. Penumbra is the region close to geometric field edges where the dose changes rapidly and depends on field defining collimators, the finite size of the focal spot (source size) and the lateral electronic disequilibrium.
3. Umbra is the region outside of the radiation field, far removed from the field edges. The dose in this region is low and results from radiation transmitted through the collimator and head shielding.

The off-axis points of the cobalt-60 beam profile are affected by:

1. The inverse square law. Dose fall-off increases as the off-axis distance increases.

2. Wedge filter angle.

Wedges are beam modifiers and serve three purposes;

1. For removing hotspots (points within patient receiving more than 100 percent normalized dose)
2. Compensates for asymmetric shape of patient body.
3. To compensate for missing tissues.

The two types of wedge filters in use are physical and dynamic wedges:

1. Physical wedge is made of lead, brass, or steel. When placed in a radiation beam, the wedge causes a progressive decrease in the intensity across the beam and a tilt of isodose curves under normal beam incidence.
2. Dynamic wedge provides the wedge effect on isodose curves through a closing motion of a collimator block during irradiation.

Physical wedges are usually available with wedge angles of 15º, 30º, 45º, and 60º. Dynamic wedges are available with any arbitrary wedge angle in the range from 0 to 60 degrees. The wedge factor is defined as the ratio of the dose rate at the reference depth for a wedged field to that for the same field without a wedge modifier. The field size dependency of the wedge factor originates from a wedge-induced increase in head scatter. The field size dependence of the wedge factor is correctly accounted for by in-air output ratios (Sc) specifically measured for wedged fields. These data are measured with the chamber axis perpendicular to the gradient direction of the wedge. Two sets of measurements should be made with the wedge in opposite orientations to ensure the correct placement of the chamber.

2.5.7 Electron contamination

Within the Cobalt – 60 energy range, photon interaction with materials can be analyzed by the photoelectric effect process, Compton inelastic scattering process and pair production process. With the monoenergetic beam of cobalt-60 of 1.25 MeV, the predominant interactions are Compton and pair production and which secondary electrons are produced from the interactions between the photon beams and the material head of the machine. These secondary electrons are termed electron contamination. These electrons are part of the primary photon beam that interacts with patient skin thereby increasing the skin dose of the patient and reducing skin sparing effect.

2.5.8 Head scatter factor

This is also known as output factor in air. The determination of the Sc is usually done by in-air measurements with sufficient material surrounding the detector to prevent contaminating secondary particles from reaching the detector volume and to provide enough charged particles for signal strength. Historically, Sc is measured at depth of maximum dose (D_{max}) with a water equivalent build-up cap and wall thickness equivalent to depth of maximum dose in water phantom (Luxton and Astrahm, 1998). This method suffers from a number of problems like detector response difference for electrons and photons, (ICRU report No. 14. 1969). Output in air varies up to 12% for open beams. Output factors in air vary an extra 5-13% for wedge beams depending on the wedge angle and location.

The value for D_{max} varies with different field sizes and source-to-surface distance (SSD) and increases with photon energy. To prevent contaminating electrons from

reaching the detector, 10 gm/cm^2 columnar mini phantoms are sufficient. In general, mini phantoms made of low-Z materials are recommended, and high-Z mini phantoms are used for small field Sc measurements. A number of studies have been reported in literature on the characteristics of Sc such as, the effect of contaminating electrons, collimator exchange effect, impact of beam-modifying devices, and the effect of source to detector distance with mini phantom and build-up cap measurements. However, the position of MLC in the treatment head is secondary or tertiary, the MLC material and the size of the material affects the Sc values.

2.5.9 Peak scatter factor.

This is defined as the ratio of the total dose and the primary dose at the depth of dose maximum (www.ncbi.com). The 'dose to small mass of medium' (DCP) is measured with just enough material around the point of interest P to provide electronic equilibrium (ionization chamber with appropriate buildup cap). At low photon energies z_{max} = zero, and the PSF is referred to as the backscatter factor. The PSF depends on field size A as well as on photon beam energy hγ and gives the factor by which the radiation dose at point P in air is increased by radiation scattered to point P from the phantom or patient.

Typical values for the PSF range from 1 for small fields of megavoltage beams, through 1.054 for a 10 × 10 cm^2 field in a cobalt beam to 1.10 for a 50 × 100 cm^2 field in a cobalt beam (used for total body irradiation (TBI)), to 1.50 for a 20 × 20 cm^2 field of orthovoltage X rays (HVL = 1 mm of Cu). While backscattering is largest at very low photon energies (classical scattering), the energy of backscattered photons is small at low photon energies, causing a rapid absorption of the scattered photons in

the medium. At intermediate and high photon energies the backscattering and side scattering decreases with energy; however, the scattered photons have a higher energy and larger penetrating power. The interrelationship between the amount of backscattering and scattered photon penetration causes the PSF first to increase with beam energy, reaching a peak around HVL of 1 mm of Cu, and then to decrease with a further increase in beam energy. The beam quality at which maximum backscatter occurs depends on field size, shifting slightly towards harder radiation with an increase in field size.

2.6 MULTILEAF COLLIMATOR (MLC) DESIGN CHARACTERISTICS

Due to intensive use of multileaf collimators (MLCs) in clinics, finding an optimum design for the leaves becomes essential. There are several studies which deal with comparison of MLC systems (Hariri et al., 2010). The three-dimensional conformal radiotherapy (3D-CRT), intensity-modulated radiotherapy (IMRT), and image-guided radiotherapy (IGRT) are the most advanced techniques in radiotherapy, which use irregular fields using multi-leaf collimators in a linear accelerator. The accuracy of these techniques depends on dosimetric characteristics of the multileaf collimators. There is an option for optimizing the jaws to the irregular MLC field to reduce the scattered radiation and intra- and inter-leaf radiation leakage beyond the field (Kotb et al., 2013).

The Multileaf collimator (MLC) has movable leaves, or shields, which can block some fractions of the radiation beam, typical MLCs have 20 to 120 leaves, arranged in pairs (Toossi et al., 2014).

Multileaf collimators are reliable, as their manufacturers developed various mechanisms for their precision, control and reliability, together with reduction of leakage and transmission of radiation between and through the leaves (Jeraj and Robar, 2004).

2.7TREATMENT PLANNING TECHNIQUES

2.7.1 Conformal Radiotherapy

Conformal radiation therapy is a geometric shaping of the radiation beam that conforms with the beam's eye view of the tumor (Gadza and Coia, 2004).

Conformal radiotherapy permits the delivery of a radical dose of radiotherapy while limiting the dose to normal tissue structures, thus minimizing the adverse effects of treatment. Its principal benefit therefore is to patients who are to be given potentially curative radiotherapy. Where radiotherapy is being given with palliative intent the prescribed total doses are usually lower and the adverse effects of palliative radiotherapy are therefore likely to be less. For this reason conformal radiotherapy is not often used when delivering palliative treatment, although it is always desirable to minimize the volume of non-target tissue that is irradiated (IAEA TECDOC-1588, 2008).

The first essential element of conformal therapy is the outlining of the patient, the target, and any organs of interest as three-dimensional structures in the correct geometrical relationship to each other. In practice, this is usually achieved using a computed tomography study. The second element is the positioning of the radiation

beams in three dimensional spaces to match optimally the beams to the target shape, to minimize the treated volume, and to keep doses to critical organs within limits. This involves the use of blocked beams and non-coplanar beams. The third element is to prescribe a higher target dose wherever possible. There is evidence that escalation of dose can be implemented without excessive morbidity, but clinical trials are required to demonstrate what clinical improvement can be achieved (Williams and Thwaites, 1993).

2.7.2 Intensity Modulated Radiotherapy (IMRT)

Radiation therapy has gone through a series of revolutions in the last few decades and it is now possible to produce highly conformal radiation dose distribution by using techniques such as intensity-modulated radiation therapy (IMRT) (Xing et al., 2006).

Intensity-modulated radiation therapy (IMRT), an extension of conformal therapy, allows for shaping of the intensity of the radiation beam. This is an important improvement, especially when the target is not well separated from normal tissues. With intensity-modulated radiotherapy (IMRT) a dose distribution can be tailored to the target volume and with improved position verification technology it is guaranteed that the dose is indeed deposited in the right place (Topolnjak, 2005).

A uniform dose distribution can be created around the tumor by either modulating the intensity of the beam during its journey through the linear accelerator or by the use of multileaf collimators (Gadza and Coia, 2004).

The clinical use of IMRT has grown rapidly as computer power increases and costs decline and several types of IMRT delivery are now becoming standard in radiation oncology hospitals. Dynamic conformal therapy with multileaf collimators is being used routinely in hospitals. With this approach, collimators conform to the tumor volume with the beam on while the treatment unit is rotating around the patient. With IMRT it is possible to shape the dose distribution to the anatomical and biological characteristics of the tumor, a concept called dose painting (Ling et al., 2000; Webb, 2001b; Topolnjak, 2005).

2.7.3 Image Guided Radiotherapy (IGRT)

Image-guided radiation therapy (IGRT) uses advanced imaging technology to better define the tumour target and is the key to reducing and ultimately eliminating the uncertainties (Xing et al., 2006). Its potential is being explored clinically using a cone-beam CT mounted on an accelerator (Jaffray et al., 1993;Topolnjak, 2005).

Image-guided radiation therapy (IGRT) uses imaging to provide images of the cancer site. Being able to see the site provides highly precise and accurate delivery of the radiation. The radiation oncologist can create and view images of the tumor site before and during the time the radiation is delivered.

IGRT is especially useful for cancer sites in parts of the body that move (such as the lungs) or for sites near major organs and tissues that should not receive radiation (like the heart or kidneys).

2.7.4 Volumetric Arc Therapy

Volumetric modulated arc therapy (VMAT) is a novel extension of conventional intensity-modulated radiotherapy (IMRT), in which an optimized three-dimensional dose distribution may be delivered in a single gantry rotation. VMAT is the predecessor to RapidArc (Popescu et al., 2010).

With volumetric modulated arc therapy (VMAT), single or multiple radiation beams sweep around the patient, greatly reducing treatment time compared to conventional radiation treatment. This new technology also offers the radiation oncologist more control and flexibility to deliver a carefully targeted dose so that only the tumour receives a high dose of radiation. Three-dimensional imaging technology aids in the precision of the radiation, giving the doctor the ability to see the tumour at the time of treatment.

CHAPTER THREE

MATERIALS AND METHOD

3.0 INTRODUCTION

This chapter outlines the materials and methods used for the research work. The design and fabrication of manual multi-leaf collimator and the procedures used to conduct the research work are also discussed.

3.1 MATERIALS

High carbon steel alloy, the material of choice for the leaf construction in this research as shown in Plate 3.0, has outer dimensions of 31 cm x 35 cm, mass of 2200 kg and density of 3.38×10^{5} kg/m^3.

The Cirus cobalt- 60 teletherapy machine (Plate3.1) was used for the quality control and dosimetric measurements on the fabricated multi-leaf collimator. A PTW 2D array detector (Plate 3.3) was used to obtain the dose profiles on the MLC. Other materials used were the thimble ionization chamber (Plate 3.2 a) and its electrometer, barometer and thermometer (Plate 3.4), a solid water phantom (Plate 3.2 b) of dimensions 20 cm × 20 cm with a 5 cm depth bore for the insertion of the ionization chamber. Below is a detailed description.

Plate 3.0 High carbon steel alloy used for the fabrication of the MLC

3.2 COBALT - 60

Cirus cobalt- 60 teletherapy machine is an isocentric teletherapy cobalt unit. The system incorporates the following features, minimum field size of 4 cm x 4 cm, availability of collimator, couch, gantry, upper and lower symmetric jaws, weight of couch 130 kg and reference distance set up of 80 cm source-to-skin distance (SSD).

The equipment is licensed to hold cobalt-60 (^{60}Co) radionuclide with 2cm diameter contained in a stainless steel shell filled with lead and natural uranium. It is designed to load cobalt-60 source of maximum activity of 228.0 TBq (10785 Ci). Plate 3.1 shows the cobalt- 60 teletherapy machine in use at the Komfo Anokye Teaching Hospital Radiotherapy Centre. A two way air cylinders using compressed air operates the source drawer. It is used to drive the source from fully shielded position (beam off condition) to a fully exposed position (beam on condition). The two (2) jaws of this collimator move together in X, Y directions from zero position to the maximum

opening. The jaws are symmetric. The maximum symmetrical field size achievable with the device is 32 cm x 32 cm at SSD 80 cm.

Plate 3.1 Cobalt- 60 teletherapy machine in use at the KATH Oncology Department

3.3 A FARMER IONIZATION CHAMBER

The field ionization chamber used for the project is a farmer type manufactured by PTW Freiburg with model number W-30010 and serial number 129 (Plate 3.2a) in a water phantom (Plate 3.2b). Its absorbed dose to water calibration coefficient ($N_{D,W}$) was used in conjunction with absorbed dose to water based protocols (i.e. TRS-398) to determine absorbed dose to water in clinical beams and the reference check source measurements. Its calibration was performed by the substitution method using the IAEA reference standard chamber NE-2561/NPL (#321). The calibration coefficients were established at the following conditions; Temperature T (20.0^0C, Pressure P (101.325kPa) and Relative Humidity R.H. = 50.0%. Its $N_{D,W}$ was 5.3nC. A pictorial view of the ionization chamber is shown in Plate 3.2a.

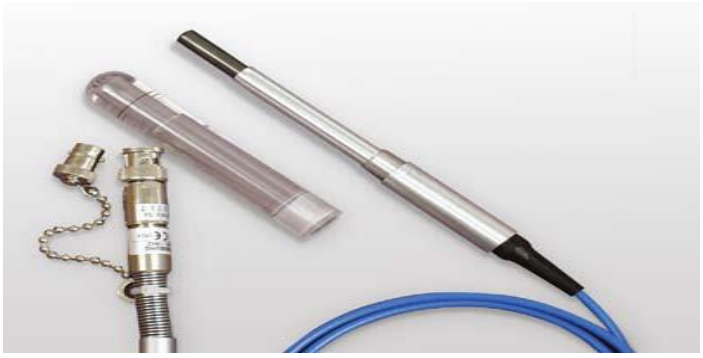

Plate 3.2a Thimble Farmer Chamber

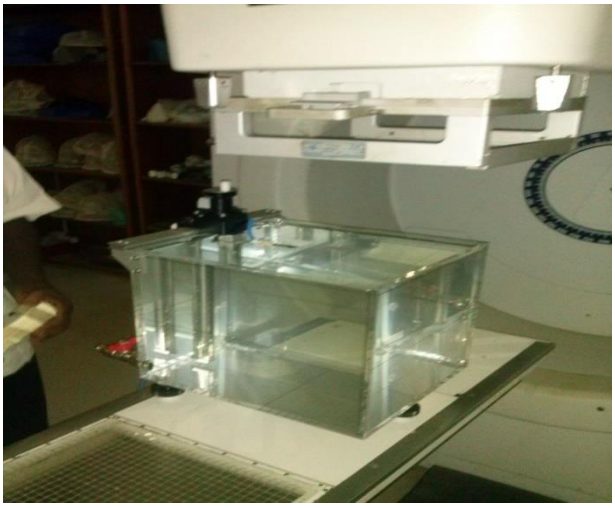

Plate3.2b Solid water phantom

3.4 PTW 2D ARRAY

A PTW 2D array (Plate 3.3) is a detector matrix with 676 diodes for quality control and dosimetry in radiation therapy.

The 2D diode array is characterized by 26 x 26 diode matrix resulting in an effective measuring field of 26 cm x 26 cm. It can be used in a slab phantom due to the flat design and records dynamic and static fields in just one run of dose or dose rate measurements. The diode was used to avoid detector ageing effects.

The PTW 2D-ARRAY is a new concept of a diode matrix in a plane for IMRT verification and quality control in radiation therapy. Utilizing ion chambers avoids radiation defects, the major drawback of solid-state detectors. The vented plane parallel ion chambers are 5 mm x 5 mm x 5 mm in size, and the center-to-center spacing is 10 mm. In total there are located 676 diodes in a matrix 26 x 26, providing a maximum field size of 26 cm x 26 cm. The surrounding material is acrylic (PMMA).

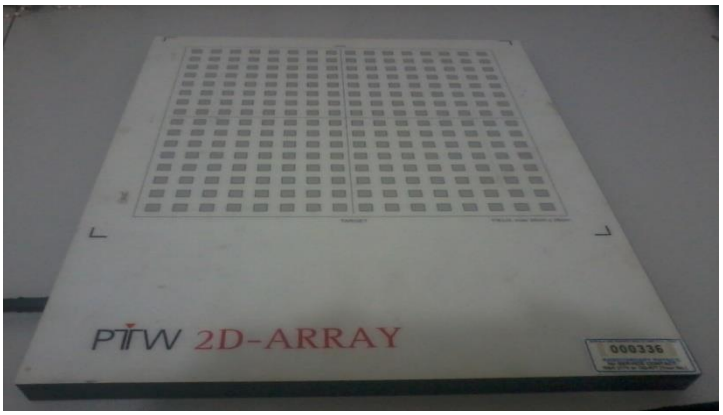

Plate 3.3 PTW 2D- Array

3.5OTHER MATERIALS INCLUDE

Digital thermometer (-40ºC to 200ºC EXTECH instruments 39240, Plate 3.4a) ,barometer S/N L991133, plate 3.4b) and a solid water phantom which has dimensions 20 cm by 20 cm with 5 cm deep bore for the insertion of the ionization chamber were used for the setup.

Plate 3.4a Digital thermometer

Plate 3.4b Barometer

3. 6 QUALITY ASSURANCE/QUALITY CONTROL

It is required that before any measurement is done clinically, quality control test should be performed. Thorough quality controls (reference check source, absolute dose to water, leakage and time error measurements) were performed on all equipment and before taking any measurement, all the equipment were allowed to acclimatize to the room's conditions.

In order to remove all traces of stray charges and check for stability, the chamber was pre-irradiated for sometime (250s to remove traces of stray charges and for stability check).

Using a reference standard system consisting of a thimble farmer type ionization chamber placed at a depth of 5 cm within the solid water phantom and connected to an electrometer readings were recorded when the chamber was irradiated by the ^{60}Co source.

The measurement was done as shown in Plate 3.5 at reference setup where the beam central axis of a standard field size of 10 cm x 10 cm coincided with that on the solid water phantom at SSD of 80 cm (Table 4.2, Appendix –I, II, and III).

To account for recombination, four (4) consecutive electrometer readings were taken for polarities of +400, -400V, +200V, -200V and 100V by setting an electrometer time of 60 seconds for each voltage.

Plate 3.5 Practical setup of the QC measurement with solid water phantom.

3.7 DOSIMETRY MEASUREMENTS WITHOUT MLC

To ensure the proper functioning and acceptance of the multi-leaf collimator, ion chamber and the electrometer, quality control measurements were done as well as dosimetry measurements for various factors. These were:

1. Percentage depth dose. Dose measurements were done in water with the Farmer ionization chamber (0.125cc), since water is equivalent to human tissues concerning radiation scattering and absorption.

2. Total scatter factor; dose and output factor were measured at a depth of 5 cm to 10 cm in increments of 1 cm. A water phantom was used with varied range of field sizes of 5cm x 5cm to 32 cm x32 cm.
3. Output factor; the output in air for a given field size to that of various sizes were measured with the ion chamber.
4. Beam profiles and wedge fields; various wedges were used for measurements. Wedges were placed on the gantry with the various field sizes measured after irradiation.
5. Head scatter factor; head scatter factor measurement was done in air with a build up cap (Perspex) surrounding detector to prevent contamination. Water phantom was used at depth of Dmax with water equivalent build up cap.

3.8 TRANSMISSION FACTOR

Any beam modifying device placed in the path of the treatment field attenuates the beam and also reduces the dose to the patient. Transmission factor is used to calculate the dose received through the shielding material. A transmission factor for the steel alloy used for the fabrication of the multi-leaf collimator (MLC) has been obtained.

According to Washington and Leaver, 2010 attenuation factor is generally represented as C_{attn} and the formula that is used to obtain transmission factor is:

$$C_{attn} = \frac{Dose\ with\ the\ block\ in\ the\ path\ of\ the\ beam}{Dose\ without\ the\ block\ in\ the\ path\ of\ the\ beam}$$

Without the steel alloy in the path of the beam, the radiation beam was on and measurements were taken with the ionization chamber (0.600 cm^3) inside the solid

water phantom and connected to the electrometer. Four consecutive readings were taken from the electrometer and recorded (Appendix – VIII).

Cirus Cobalt- 60 teletherapy machine was used to measure the transmission factor with mean energy of 1.25 MeV and 10 cm x10 cm field size at 80 cm source to skin distance (SSD).

3.9 METHODOLOGY

The initial design format and characteristics, and fabrication were done at the radiotherapy department of Komfo Anokye Teaching Hospital using these procedures;

1. Solid triangular grooves which overlap each other perpendicularly were chosen over curved grooves and tongues for their ease of movement and ease of fabrication.
2. Later analysis and alterations were done with the initial design changed to solid tongue and groove shape as shown in Plate 3.6
3. Detailed measurements of the original Cirus cobalt-60 collimator frame dimensions were done to help in getting accurate dimensions for the prototype under consideration.
4. Styrofoam and wood were used as initial model materials in place of steel alloy to help correct mistakes and outline the perfect design to consider.

3.9.1COLLIMATOR DESIGN AND CONSTRUCTION (PROTOTYPE)

MLCs were designed to fit exactly into the head of the linear accelerator. The Varian model of fabrication was chosen as the main design. After the initial dimensions of the original collimator were taken, Styrofoam was chosen as the sample substance to

help in the design process. The Styrofoam was cut to the shape of a leaf, which consisted of ten pairs with each leaf having a width of 7 cm, a thickness of 6 cm and length of 16 cm at the isocenter to produce a maximum field size of 32.5 cm x 32.5 cm. It consisted of 10 leaves on each side of the frame lying perpendicular to each other to create a leaf bank capable of been adjusted to conform to any shape and size under consideration of the 32 cm x 32 cm field size. The collimator leaf frame (Plate 3.7) could not be designed with the Styrofoam but presented an idea as to how to go about constructing it. It is in such a way that each leaf can be moved individually and manually to match each patient's specific treatment plan. The wooden MLC prototype (Plate 3.9 a, b) was then sent to the mechanical engineering shop for the fabrication of the multi-leaf collimator (MLC). Steel alloy was preferred to other metals due to its compatibility with other elements and improved mechanical properties wear resistance, corrosion resistance and harden ability.

Plate 3.6a. Initial styrofoam designs to mimic the original collimator "leaves".

Plate3.6b. Initial Styrofoam designs to mimic the original collimator “leaves”.

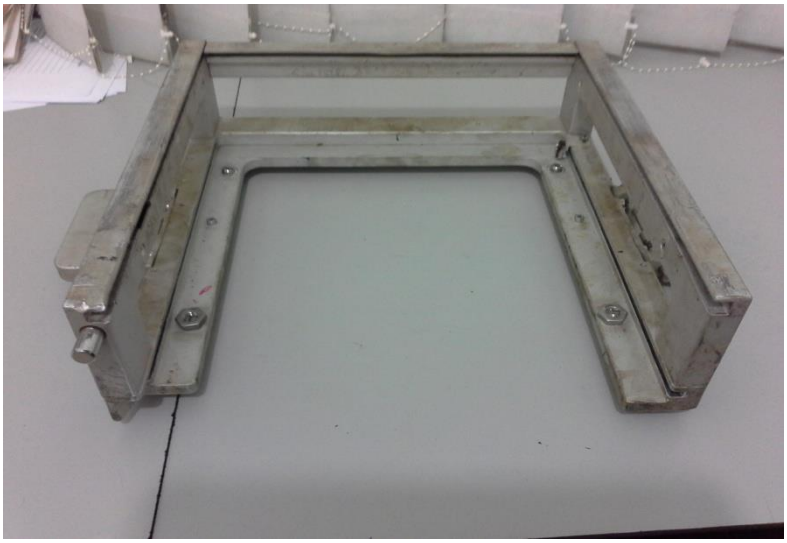

Plate3.7.Multi leaf collimator frame.


(a)


(b)

Plate3.8.Modelled multi-leaf collimator (initial) opened to a desired field size (a) and the final collimator design (b).

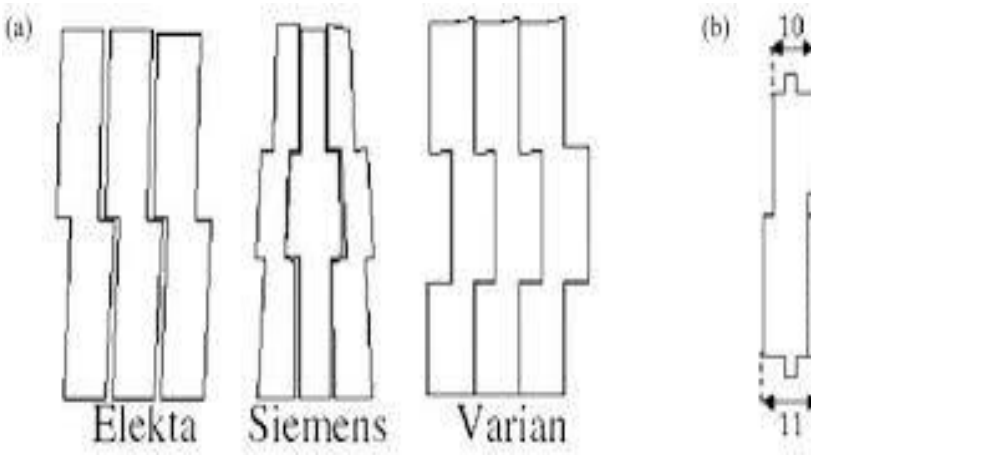

This Work

Plate3.9 (a) shows the individual leave designs of the types of the MLC which were considered. (b) schematic diagram of the suggested leaf design.

3.9.2 MLC LEAF MODEL FABRICATION

The steel alloy metal was initially cut into block forms by using a gas cutter. This was done to make the leaves nicer and smoother. Plate 3.10 shows the picture of the blocks formed.

The blocks were then sent to the lathe machine (Plate 3.11) to make the block smooth and brighter so that the shape of the MLC will be designed perfectly. The fabricated MLCs (Plate 3.12a, b and Plate 3.13) consist of 4 pairs of leaves. Each leaf has a mass of 5 kg, width 7.5 cm, height 6 cm and length of 16 cm producing maximum field of 32 cm x 32 cm at the isocentre. The leaf frame designed to hold the leaves (Plate 3.14) has a weight of 7 kg with total weight of 47 kg.

3.9.3 MLC Control Features

MLCs produced by different manufacturers employ different mechanisms for moving the leaves accurately to their prescribed positions. The task of moving a leaf to the correct position normally depends on the mechanism that moves the leaf to position. In this work, a novel drive mechanism for the individual leafs has been implemented by using screws. This is in contrast to motors or active pneumatic systems as in commercially available binary MLC.

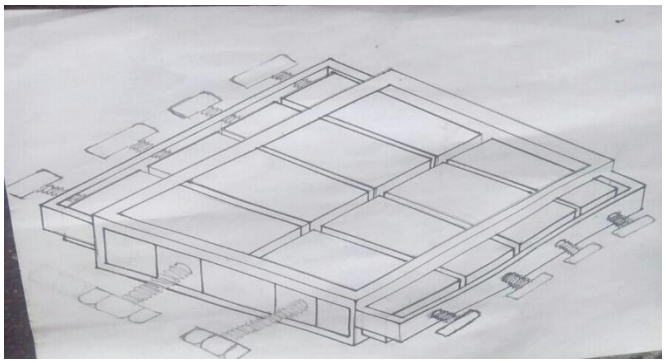

Plate 3.10a Technical drawing of the MLC

Plate 3.10b Picture of the blocks formed

Plate 3.11: Lathe machine used for the fabrication of the MLC

Plate 3.12 Picture of the smoothed blocks by the lathe machine

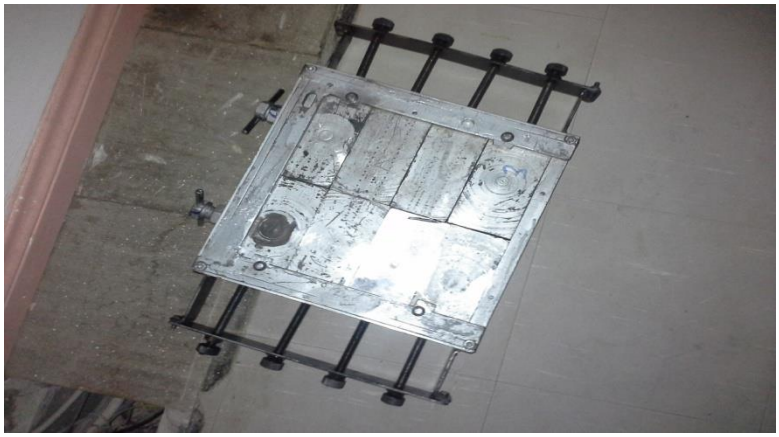

Plate 3.13a Fabricated MLC

Plate 3.13b fabricated MLC fixed onto the Cirus Cobalt-60 head

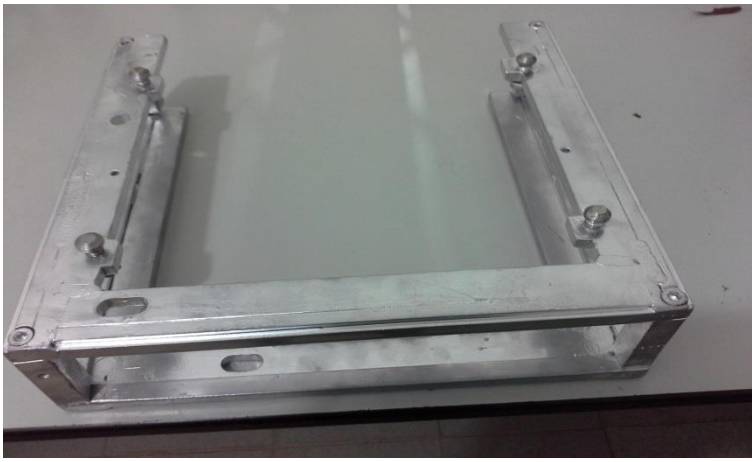

Plate 3.14 Leaf frame designed to hold the leaves locally

3.10 DOSIMETRY MEASUREMENT WITH THE FABRICATED MLC

3.10.1 Beam profiles for open and closed MLC fields

In external beam radiotherapy, transverse and longitudinal dose measurements are taken with a radiation detector in order to characterise the radiation beams from cobalt-60 teletherapy machines and linear accelerators. Photon beams may be represented as a depth dose chart (along the central beam axis), a beam profile (perpendicular to the beam axis), or an isodose chart (a plane parallel or perpendicular to the beam axis).

In measuring the beam profile for open MLC fields, the MLCs were opened to the full range of the field. This was done to take the measurements in air. The MLCs were also closed and measurements were taken using the PTW 2D- array detector and the cobalt-60 teletherapy machine. Measurements were taken from 0 to 15 cm depths with various field sizes of 4 x 4 to 32 x 32 cm^2. Plate 3.15 shows the practical setup used in this work for the beam profile measurement. This measurement was done to check for leakage through the leaves. Leakage through the MLC consists of transmission

through the leaves and the leakage between the leaves. Leakages through the leaves were determined by the PTW 2D array with the PTW-2D software Version 1.00.

Plate 3.15 Practical setup used in this work for the beam profile

3.10.2 Output Factors

Output of the Cirus ^{60}Co machine is the dose monitored using a calibrated ion chamber in the head of Cirus ^{60}Co machine and calibrated to give 1cGy/mu at 80 SSD and for 10 x10 cm^2.Output factor as defined by Khan (1984) is also known as collimator scatter factor (Sc) which is the ratio of output in air for a given field to that for a 10 x 10 cm^2 field this is measured by a calibrated ion chamber. As the output factor is the product of the collimator scatter corrections factor and the phantom scatter correction factor, the phantom scatter correction factor may be found by dividing the output factor by the collimator correction factor. In this work, the output factors were measured at a reference source to surface distance SSD at 80 cm. Measurements were then taken at various field sizes from 4 cm x 4 cm to 32 cm x 32

cm by varying the depths of 0.5 to 15 cm in steps of 0.5 cm. Plate 3.18 shows the practical setup for the output factors measurements.

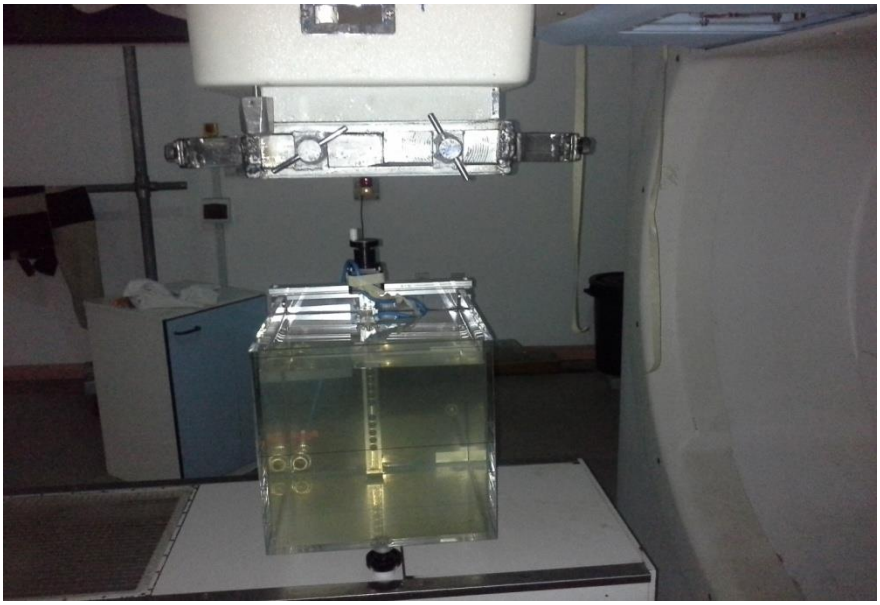

Plate 3.16 Practical setup for the output factors

3.10.3 Multi-leaf Collimator (MLC) Effect

For these measurements the MLC was used to define fields from 7.5 cm x 7.5 cm to 15 cm x 15 cm with square and rectangular field sizes (23 cm x 15 cm, 23 cm x 20 cm). With the upper and lower jaws set to various field sizes (4 cm x 4 cm to 32 cm x 32 cm), the ion chamber and the water phantom, were used to take readings. After, the MLC was set from 7.5 cm x 7.5 cm to 15 cm x 15 cm and varying the field sizes and at a depth through 0.5 cm to 15 cm measurements were taken to ascertain the effect of the MLC and the collimator jaw settings.

3.10.4 Beam Profile of MLC

The distribution of dose at any point within a radiation beam is required to be known for treatment planning. Beam profiles are measured to characterize the dose at points off the central axis.

This test was done by opening the MLC to a field size of 15 cm x 15 cm. It was performed by using PTW 2D array and the jaw settings of 32 cm x 32 cm. Plates 3.17a &b show the opening of the MLC to a set field size.

Plate 3.17a MLC set to 15 cm x 15 cm field size

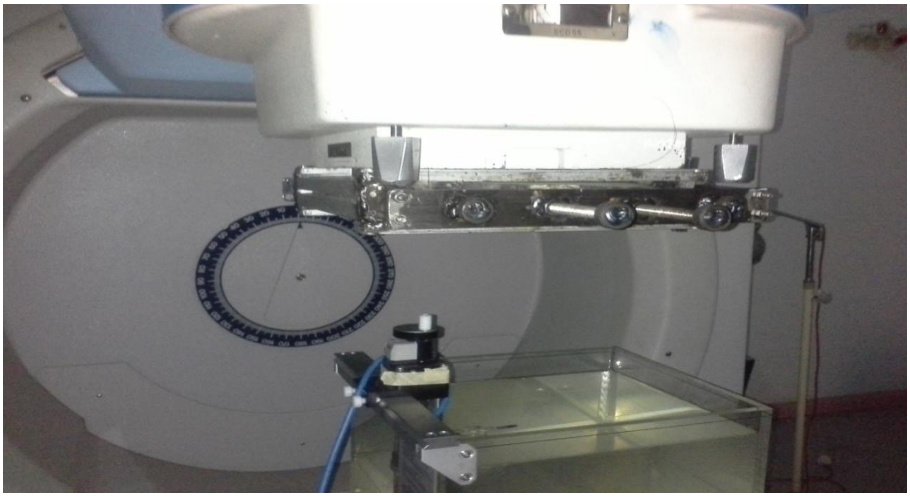

Plate 3.17b MLC of field size 15 cm x 15 cm

3.10.5 MLC Transmission

Transmission through the MLC was determined with ion chamber measurements in a water phantom. A cylindrical chamber (0.125 cubic centimetre) was placed at 80 cm source to surface distance on the central axis. Measurements were made for fields defined by the upper and lower jaws, with the MLC in the open and closed positions. The ratios of these measurements determine the transmission factor (Table 4.1, Appendix-V). The MLC was closed in order to avoid leakage between the leaf ends.

CHAPTER FOUR

RESULTS AND DISCUSSIONS

4.0 INTRODUCTION

The chapter presents and discusses the results obtained from the study. It describes the various results for the quality control, the MLC dosimetry measurements and the various results obtained with graphs. Results for leaf transmission factor, reference check source measurements, absorbed dose to water determination using TRS 398 protocol, percentage depth dose, beam profiles for open field and wedge fields, beam profiles for open and closed MLC fields, MLC effect, total scatter factors, collimator and scattering factors and output factor.

4.1. TRANSMISSION FACTOR

Transmission factor for a multileaf collimator is a basic requirement for selecting a suitable material. Table 4.1 shows various materials and their respective transmission factors that were used for the research.

Table 4.1: Various materials and their transmission factors

Material	Thickness (cm)	Transmission Factor (%)
Mild Steel	5	16.2
High Steel Carbon	7	4.18

4.2 QUALITY CONTROL MEASUREMENTS

4.2.1 Reference check source measurements

The stability of the chamber is critical in accurate measurements. A long – lived radionuclide (Strontium – 90) is therefore needed to measure and calculate the drift in the ionisation stability with time. The table 4.2 illustrates a typical reading of the stability and constancy of the ionisation chamber used for the measurements. Two different electrometers were used; the PTW Unidos and the NE2670 Farmer Electrometer. The variation between the two electrometers was of the order of 1.34 percent.

Table 4.2: Reference check source measurements for rdgy 420 examinations using a chamber calibrated in terms of N_{DW} practical data.

No.	**Time: t [s]**	**Reading [nC] UNIDOS E**	**Reading [nC] NE2670 FARMER CHAMBER**
1	250	2.806	2.7673
2	250	2.806	2.7682
3	250	2.806	2.7685
4	250	2.806	2.7691
5	250	2.809	2.7696
Mean Q_{mean}	**250**	2.806	2.7685
Std. dev. = $\left(\frac{Max\ Value - mean}{mean}\right)$		0.001069	0.000397

The ambient conditions for the measurements are as follows:

T_{in} [^{0}C]: 22.1 P_{in} [KPa/mbar]: 97.87 Relative Humidity [%]: 29%

$$K_{in}[T,P]=\left[\frac{273.15+T_C}{293.15}\right]\times\frac{101.3}{B_S}=\frac{273.15+(22.10)}{293.15}\times\frac{101.3}{(97.87)}=1.0424612 \quad \textbf{3.2}$$

T_{fin}[^{0}C]: 23.9P_{fin} [KPa/mbar]:97.89 Relative Humidity [%]: 29%

$$K_{fin}[T,P]=\left[\frac{273.15+T_C}{293.15}\right]\times\frac{101.3}{B_S}=\frac{273.15+(23.90)}{293.15}\times\frac{101.3}{(97.89)}=1.0486022 \quad \textbf{3.3}$$

Where:

K_{in} = Initial correction factor

K_{fin} = Final correction factor

T_{in} = Initial corrected temperature

T_{fin} = Final corrected temperature

P_{in} = Initial corrected pressure

P_{fin} = Final corrected pressure

B_s =Ambient pressure

Calculations

Measured Check Source value (Q_{meas}) = $Q_{read}\times K[T,P]_{mean}$ = 2.806 x 1.0455 = 2.933

Reference Check Source measurement (Q_{quot}) = 2.886 nC 250 s^{-1} as at

Decay correction factor (f): from …31/12/15…….. to 21/01/16……;
……0.0575…… years elapsed

Therefore, f = $e^{-\lambda t} = e^{-\frac{0.693t}{T_{1/2}}} = e^{-\frac{0.693t}{28.7}} = \ldots 0.24947 \ldots\ldots\ldots\ldots\ldots\ldots\ldots\ldots$,

$T_{1/2}$ *for* $^{90}Sr = 28.7a$

.

Deviation, $\Delta = \left(\frac{Q_{meas} - Q_{quot}}{Q_{quot}} \right) \times 100\% =$ (2.933-2.886/ 2.886) x 100% **3.4**

= 1.6%

A deviation of 1.6 percent falls within the acceptable tolerance for stability and therefore the chamber used is considered stable for measurements.

4.2.2 Absorbed dose to water rate for ^{60}Co teletherapy unit using a chamber Calibrated in terms of N_{Dw} data

Measurements for the absorbed dose to water rate were done for various voltages namely +400V, +200V, +100V, -100V, -200V and -400V. These provided the platform for electrometer, polarity and recombination corrections in accordance with IAEA protocols (Table 4.3).

Using the initial temperatures, atmospheric pressures, and the relative humidity,

$$K_{in}[T,P] = \left[\frac{273.15 + T_C}{293.15} \right] \times \frac{101.3}{B_S} = \frac{273.15 + (20.00)}{293.15} \times \frac{101.3}{(97.55)} = 1.0384418 \quad \textbf{3.5}$$

Using the final temperatures, atmospheric pressures and relative humidity,

$$K_{fin}[T,P] = \left[\frac{273.15 + T_C}{293.15} \right] \times \frac{101.3}{B_S} = \frac{273.15 + (23.05)}{293.15} \times \frac{101.3}{(97.54)} = 1.0491765 \quad \textbf{3.6}$$

Table 4.3: Absorbed dose to water rate for Co-60 teletherapy unit using a chamber calibrated in terms of N_{DW} practical data.

No.	+ 400V Reading [nC]	- 400V Reading [nC]	+ 400V Reading [nC]	+ 200V Reading [nC]	- 200V Reading [nC]	100 V Reading [nC]
1	13.8	- 14.9	13.6	13.6	- 15.0	13.5
2	13.7	- 14.9	13.6	13.5	- 15.0	13.5
3	13.7	- 14.9	13.6	13.6	- 15.0	13.5
4	13.7	- 14.9	13.6	13.6	- 15.0	13.5
5	13.7	-15.0	13.6	13.6	- 15.0	13.5
6	13.7	- 15.0	13.6	13.5	- 15.0	13.5
7	13.7	- 15.0	13.6	13.6	- 15.0	13.6
8	13.7	- 15.0	13.6	13.5	- 15.0	13.5
9	13.7	- 15.0	13.6	13.5	- 15.0	14.29
10	13.7	-14.96	13.6	13.5	- 15.0	14.29
Mean M_W	13.71	14.96	13.6	13.55	15.00	13.67
Std. dev.	0.006	-1.996	0	0.004	0	0.045

Electrometer calibration factor k_{elec} : 1.00

Polarity correction rdg at +V1: 400 rdg at -V1:400

$$k_{pol} = \frac{|M_+| + |M_-|}{2M} =$$

$$K_{pol} = \frac{(13.71) + (14.96)}{2(13.71)} = \frac{28.67}{27.42} = 1.0456$$

Recombination correction (two-voltage method)

Polarizing voltages: V1 (normal) = +400V V2 (reduced) = -400 V

Readings at each V: M1 = 13.8 M2 = 14.9

Voltage ratio V1 / V2 = 400/100 = 4 Ratio of readings M1 / M2 = 13.8/13.67 = 1.0029

$$k_s = \frac{(V_1/V_2)^2 - 1}{(V_1/V_2)^2 - (M_1/M_2)} =$$

K_s = ((400/200)^2 -1)/ ((400/200)^2 – (13.8/13.6)) = 3/2.9853

= 1.004

Corrected dosimeter reading at the voltage V1:

$$M = M_1\, k_{TP}\, k_{elec}\, k_{pol}\, k_s = \quad \text{nC/min}$$

$$M = 13.71 \times 1.044 \times 1.000 \times 1.0456 \times 1.004 = 15.0258\, nC/min$$

5.33E07 Gy/C = 0.0532 Gy/nC

Calculations

Determination of absorbed dose to water rate ($_5D_{W\ meas}$)

$$_5D_{W\ meas} = M \times {}_5N_{DW} = 15.0258\frac{nC}{\min} \times 0.0532\frac{Gy}{nC} = 0.7994\frac{Gy}{\min}$$

Dose at $5cm = {}_5D_W =$

$$Dose\ at\ 0.5cm\,(d_{\max}),\ {}_{0.5}D_W = \frac{{}_5D_W}{0.788} = \frac{0.7994}{0.788} = 1.0144\,Gy/\min = 101.44\,cGy/\min$$

4.2.3 Time Error

Time error accounts for differences between timer settings and actual time the beam is ON. It is equal to the negative of the "end effect" or timer error,τ.

The timer error is most commonly determined using the multiple exposure method:

$$\text{Time error} = \tau = \frac{M_B t_A - M_A t_B}{n M_A - M_B} \qquad \textbf{3.7}$$

Multiple exposures, n, of duration t/n are made, and the integrated reading M_B is compared to the reading M_A obtained in a single exposure of duration t.

If τ is positive, the irradiation time is longer than the setting on the timer. The timer correction then requires that this time is subtracted; If τ is negative, the exposure time is shorter than the timer setting. The correction in this case requires that this time be added.

Table 4.4: Time error practical data

Type of Reading	n	Readings (nC)	Time
M_A	4	57.20	$t_A = 4$
M_B	4	57.29	$t_B = 4$

Calculation: $timer\ error,\ \tau = \frac{M_B t_A - M_A t_B}{n M_A - M_B} = 0.0021$ minutes

4.3 DOSIMETRY MEASUREMENTS DATA WITHOUT MLC

4.3.1 Collimator and phantom scattering factors data

Measurements for the collimator factor and scattering factors were done with field sizes ranging from10 cm x10 cm to 32 cm x32 cm at various depths. Using the initial temperatures, atmospheric pressures, and the relative humidity. See Appendix –II

$$K_{in}[T,P]=\left[\frac{273.15+T_C}{293.15}\right]\times\frac{101.3}{B_S}=\frac{273.15+(20.65)}{293.15}\times\frac{101.3}{(97.71)}=1.0390402 \quad \textbf{3.8}$$

Using the final temperatures, atmospheric pressures and relative humidity,

$$K_{fin}[T,P]=\left[\frac{273.15+T_C}{293.15}\right]\times\frac{101.3}{B_S}=\frac{273.15+(21.00)}{293.15}\times\frac{101.3}{(97.63)}=1.0411303 \quad \textbf{3.9}$$

The relationship between the collimator scatter factor and field size is shown in Figure 4.1. The factor increases as the field size (scatter) increases nonlinearly.

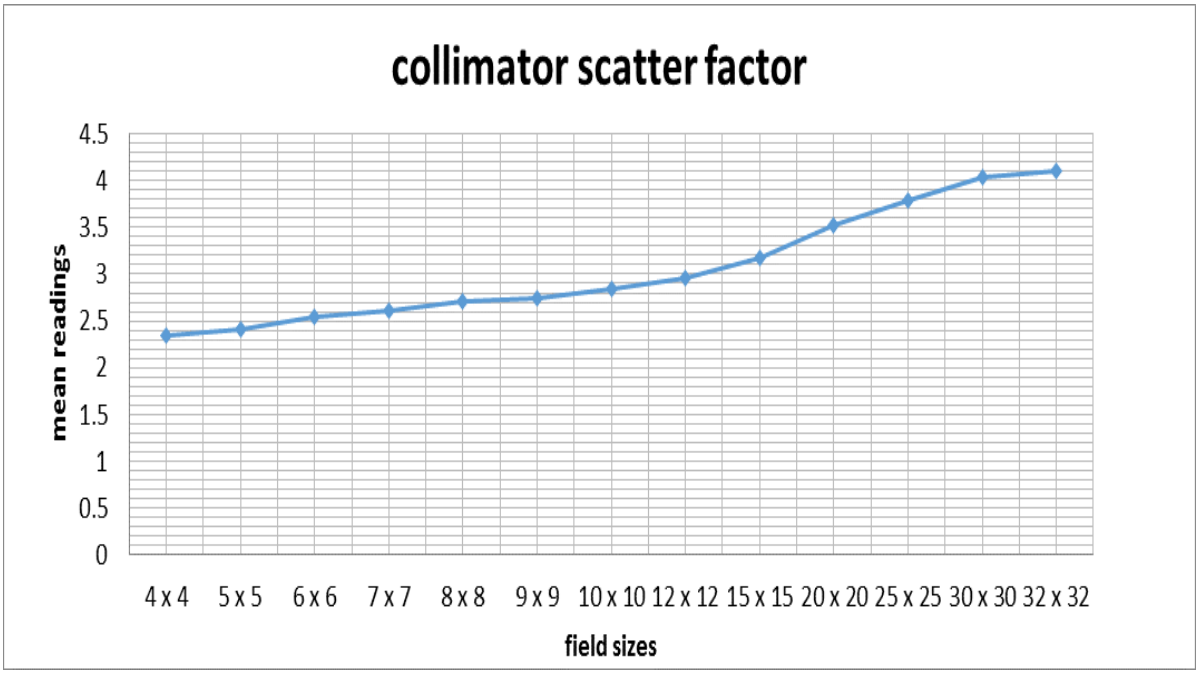

Figure.4.1. Collimator factors variation with field sizes.

4.3.2 Output factor data

Output factor is an important dosimetric factor showing the effect of scatter (field size) on absorbed dose within the patient. The CIRUS cobalt – 60 machine has a minimum field size of 4.0 x 4.0 cm^2 to 32.0 x 32.0 cm^2. Figure 4.2 shows the output factor used for determining the percentage depth dose and tissue maximum ratio.

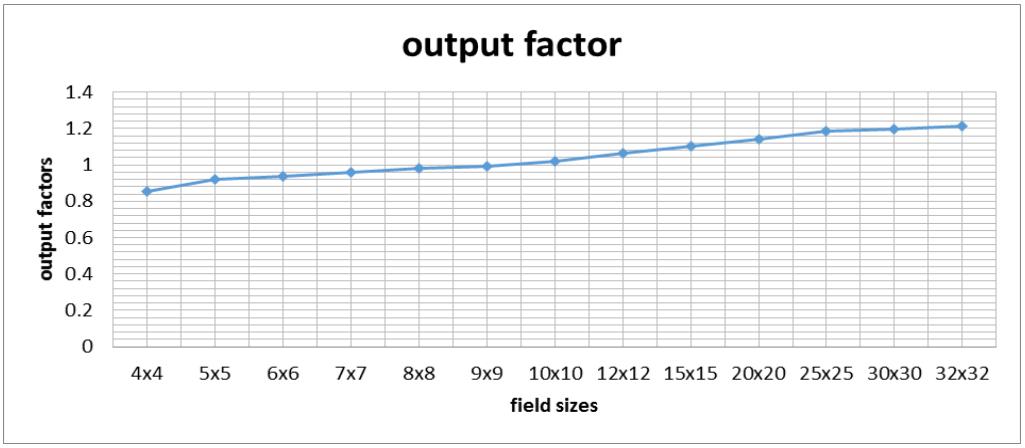

Figure 4.2 shows the output factors variations with various field sizes
From the Figure 4.2, it can be deducted that the output factors increase with increasing field sizes.

4.3.3 Beam profiles for open and wedge fields data

With respect to the orientation of patient treatment coordinates, Figure 4.3 shows the various planes for dose profiles and collimator leaf leakages. The z-axis is along the patient's head – to – toe orientation.

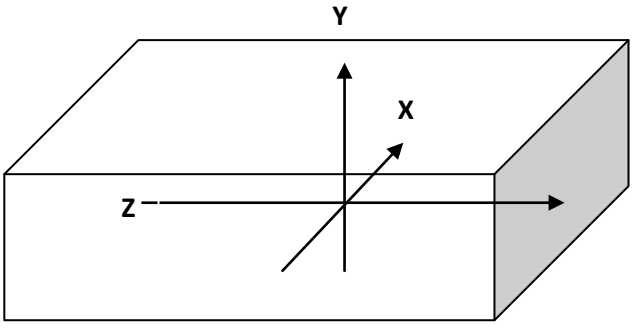

Couch

Figure 4.3 Dose profiles orientation

The PTW-2D soft V.1.00 was used to determine the profiles for the various sizes in graphical representation in 2D. The software shows both the dose profile and the dose in a coloured diagram as shown in Plate 4.0 and 4.1. The dose profile is the dose deposited in the patient with respect to depth and x-y plane of the patient. Plate 4.0 shows the dose profile for a 30 degrees wedge with 25 cm x 25 cm field size. Plate 4.1is an open 15 cm x 15 cm MLC field

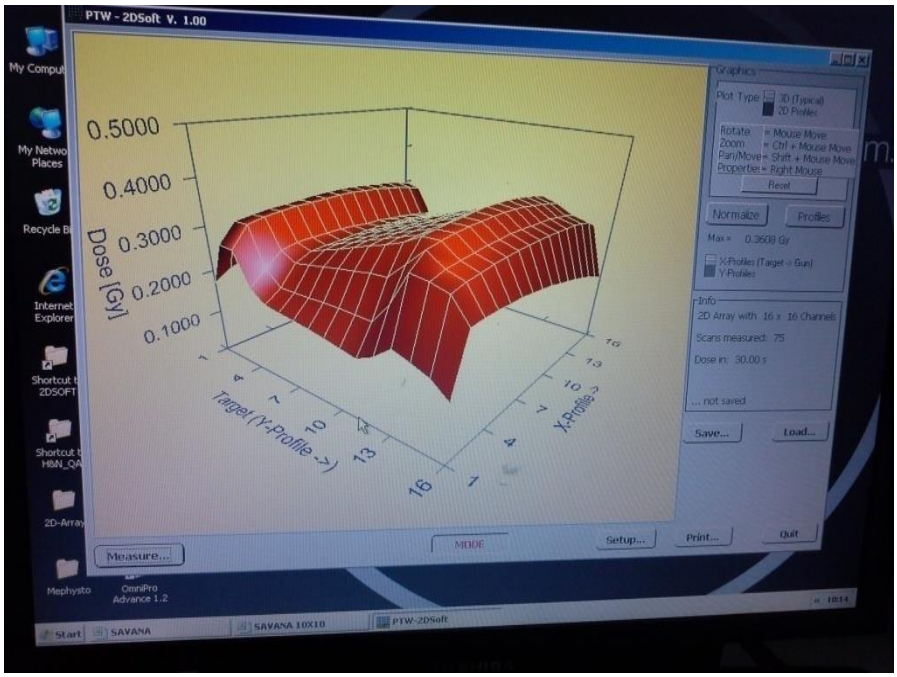

Plate 4.0. Dose profile for 30 degrees wedge of 25 cm x 25 cm field size.

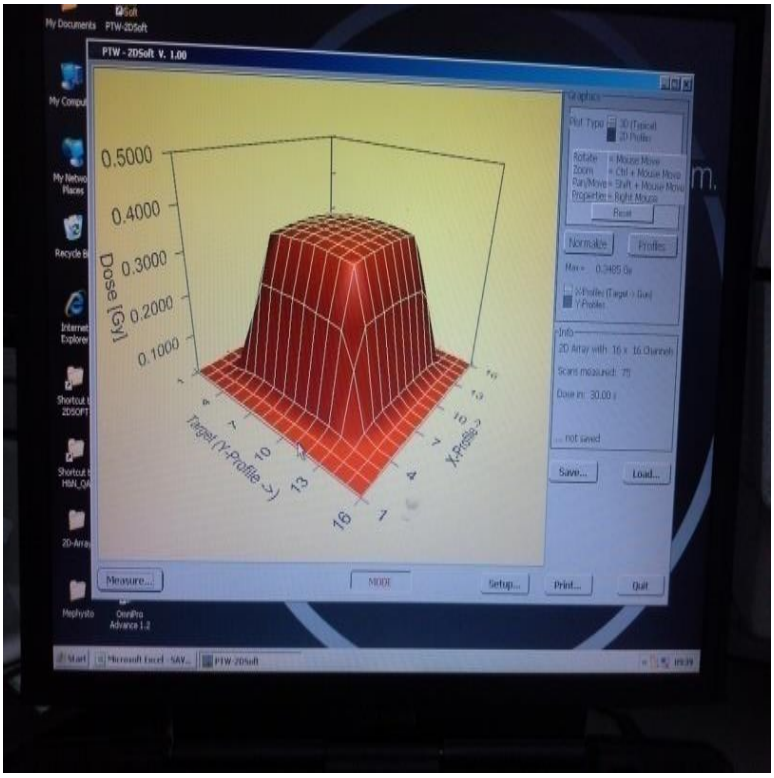

Plate 4.1.Dose profile for open field, 15cm x 15cm field size

4.4 DOSIMETRY MEASUREMENTS DATA WITH MLC

4.4.1 MLC Transmission Profiles

Transmission profiles obtained for square field sizes with varying depth from 0.5 cm to 15 cm using PTW 2D array detector are shown in Plates 4.2, 4.3 and 4.4. The transmission was found to be 4.18%

Beam profiles for open and close MLC fields were measured for square field size ranging from 4 cm x 4cm to 32 cm x 32 cm with respect to depths from 0.5 cm to 15 cm. The result of measured data is shown graphically in Plate 4.5.

The software shows both the dose profile and the dose in the diagram as shown in the examples below. The open profile data must show a flat symmetrical beam in the x

and y – directions. Plate 4.2 shows some level of asymmetrical profile confirming imperfections in the fabrication. Plate 4.4 identifies the asymmetrical effect at the edges. The beam profiles determined in this work were done for leaf leakage. From Plates 4.2 to 4.6, it was seen that leakage increases with field size. This is as a result of the leaf ends.

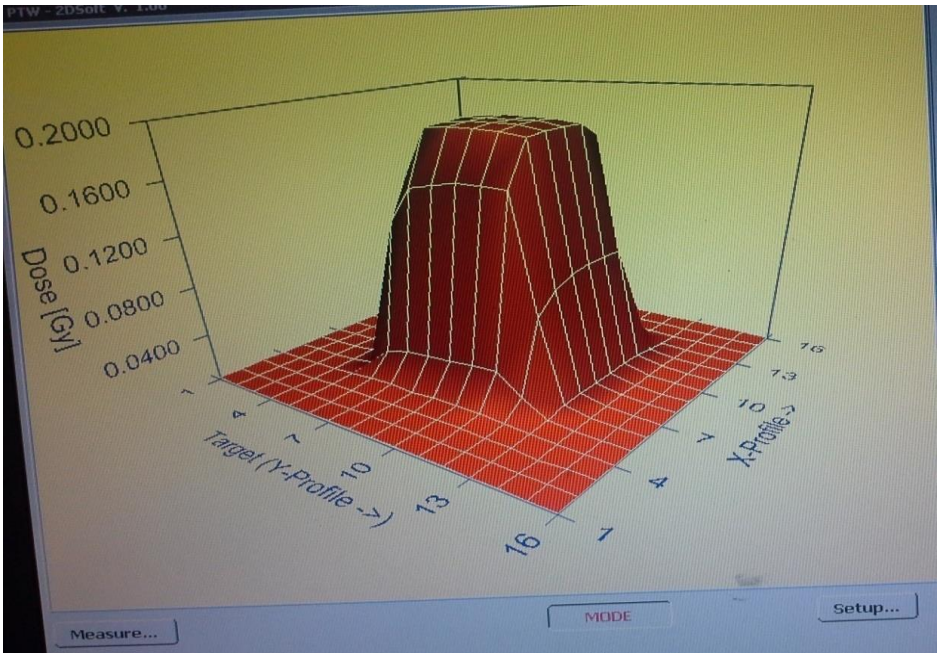

Plate 4.2Beam profile for open MLC fields of 10 cm x 10 cm field size

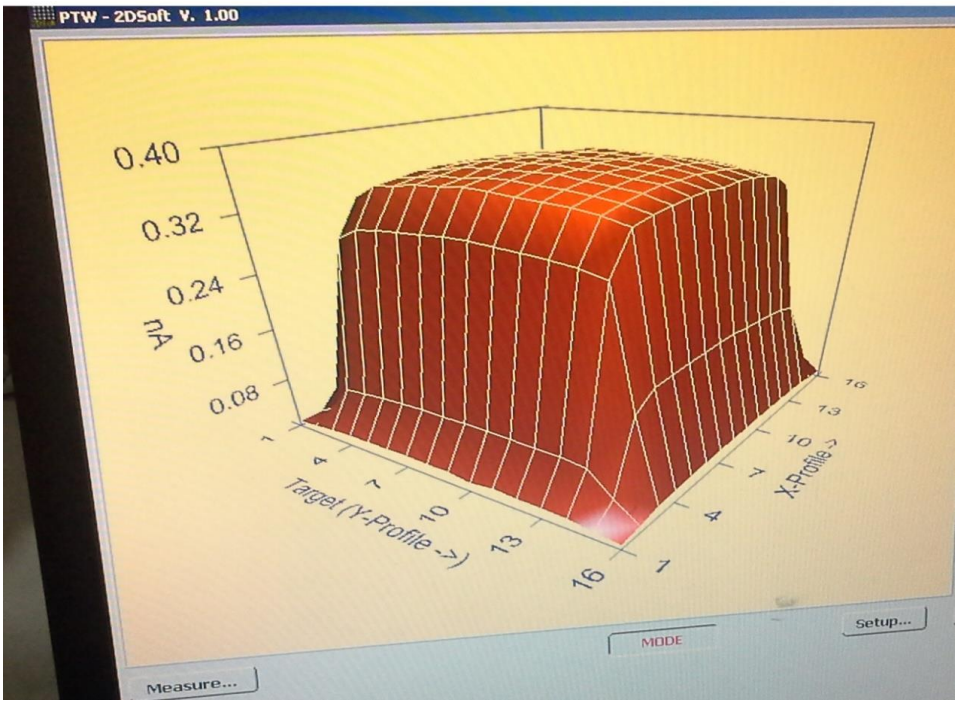

Plate 4.3 Beam profile for open MLC fields of 20 cm x 20 cm field size

Plate 4.4 illustrates the verification of the transmission of the light field and confirmed with a film test. The dose profile easily shows the leakage and therefore the transmission of light through the leaves. Plates 4.4 and 4.5 confirm that there is a gap between two leaves.

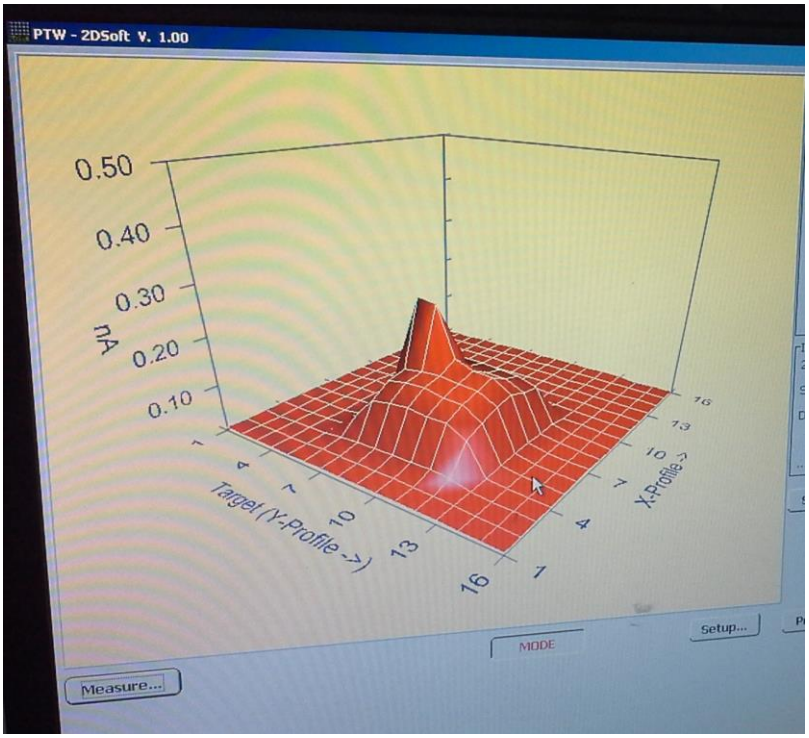

Plate 4.4 Beam profile for close MLC fields of 10 cm x 10 cm field size

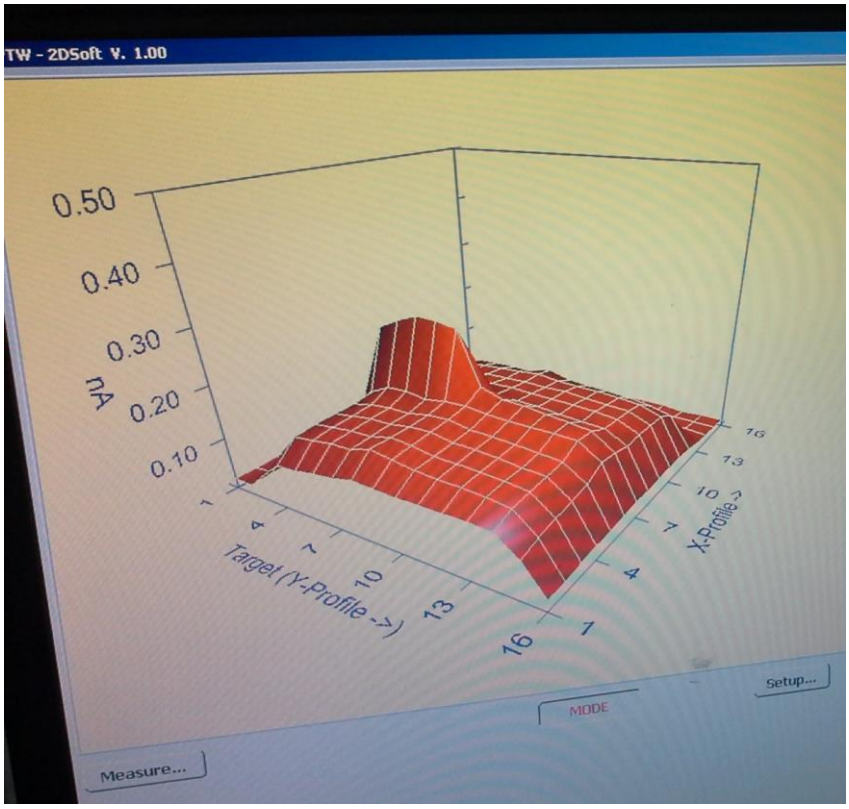

Plate 4.5 Beam profile for close MLC fields of 20 cm x 20 cm field size

4.4.2Output Factors Data

Output factors for square field size which ranges from 4 cm x 4 cm to 32 cm x 32 cm were measured with all standard protocols with varying depths from 0.5 cm to 15 cm. The results of the measured data are shown graphically in Figures 4.4.1 and 4.4.2. From Figure 4.4.1, it was seen that as field size increases output factor also increases and that was when the MLC was opened to a full range. With the closed field of the MLC, shown in Figure 4.4.2, as the leaf window moves across the target, each point in the target seems to overlap.

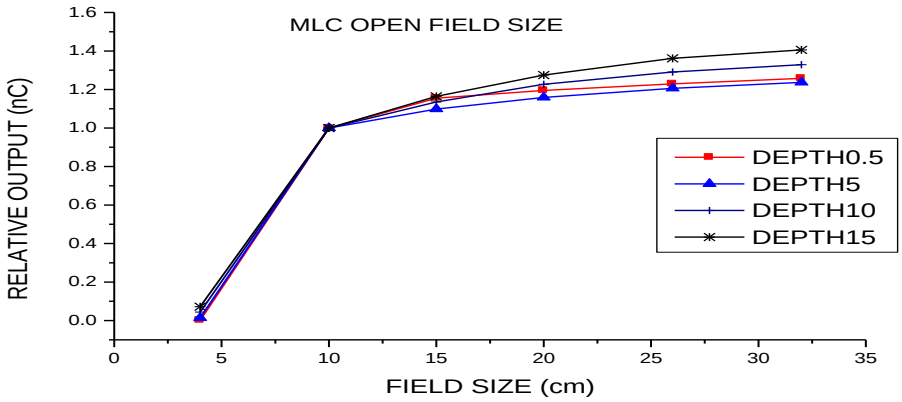

Figure 4.4.1 MLC open field for square field size

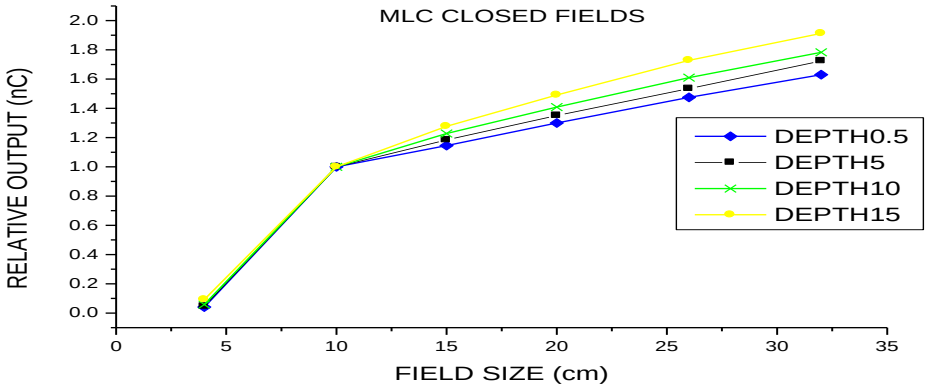

Figure 4.4.2 MLC closed field for square field size

4.4.3Multileaf Collimator Effect Data

Multileaf collimator (MLC) effect was measured for the opening of the MLC of field sizes 7.5 cm x 7.5 cm and 15 cm x 15 cm. MLC effect is comparing the same field size for open field to that of the MLC. The results are shown graphically on Figure4.5.1 and 4.5.2. From Figure 4.5.1, it was seen as the field size increases, the depths from 5 cm to 15 cm seems overlapping. But from Figure 4.5.2, the depth of 0.5 cm looks open from the other depths. This is due to scatter.

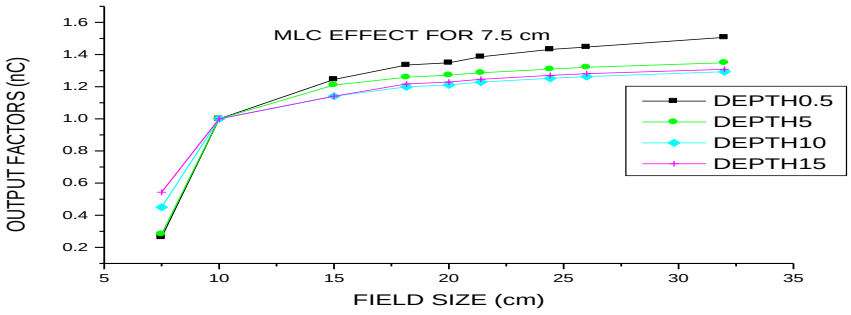

Figure 4.5.1 MLC effect for 7.5 cm x 7.5 cm field size

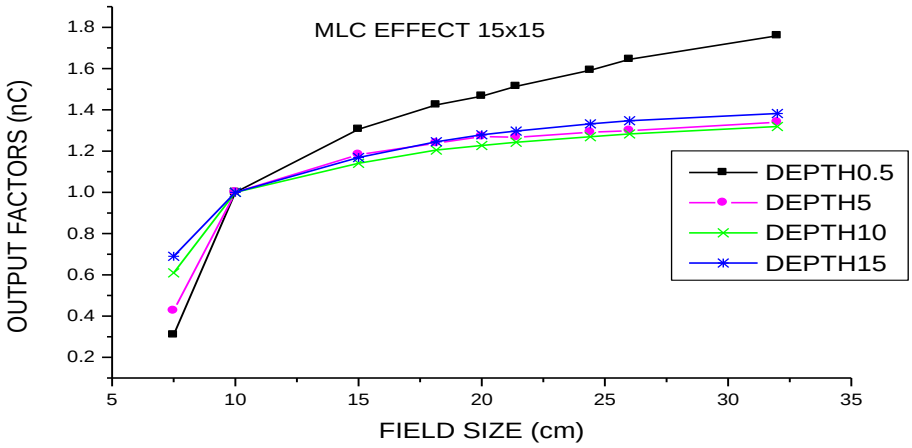

Figure 4.5.2 MLC effect for 15 cm x 15 cm field size

4.4.4 Beam Profile of MLC Data

Beam profile of MLC was measured for a square field size of 32 cm x 32 cm.

Plate 4.7 shows the result for the beam profile of MLC.

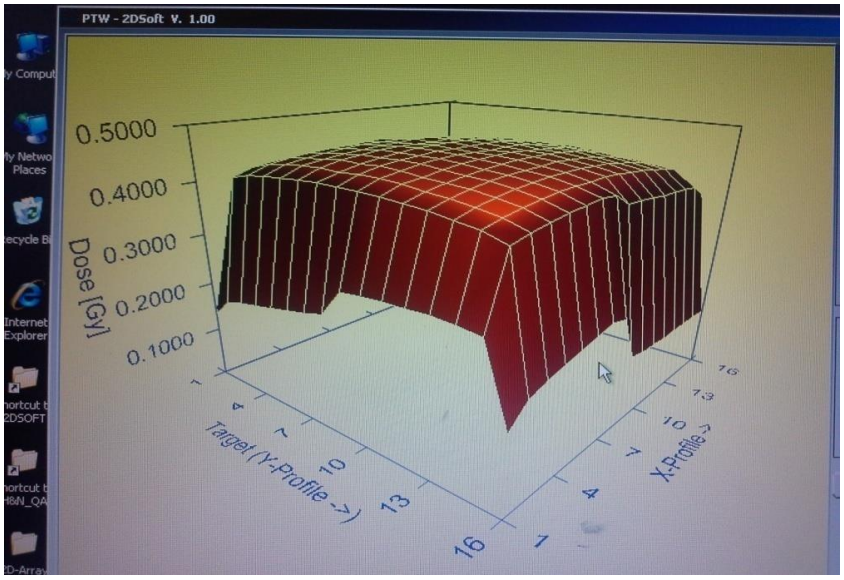

Plate 4.7 Beam Profile of MLC

CHAPTER 5

CONCLUSION AND RECOMMENDATIONS

5.1 CONCLUSION

The multileaf collimator fabricated can be used for square and rectangular fields. It can also be used to treat a small field size as well as irregular fields. The dosimetric properties determined were output factors for open and closed MLC fields, beam profiles for the MLC and the collimator jaws, the MLC effect and the leaf transmission. Leakage was determined with the dose profile. Leakage was high as the field size increases due to the design of the leaf ends. The beam profiles were determined for open MLC field and closed MLC field. The transmission factor for the steel alloy was found to be 4.18%. The transmission of the leaf was also determined to be 4.8%, which all falls within the accepted value of 5% for custom blocks and MLC. The leaves and the leaf frame of the MLC were initially constructed using Styrofoam, wood as the final prototype, and high carbon steel as the final MLC model. Output factors were measured to determine the leaf transmission. As the field size increases output factors also increase. With the closed field of MLC, as the leaf window moves across the target, each point in the target seems to overlap. By using PTW 2D array detector, MLC effect measurements were done. MLC effect measurements were done to ascertain the effect of the MLC and the collimator jaw settings. The fabricated MLC shows promising results in the field of conformal radiotherapy and reliability of its performance to meet dosimetry and accuracy requirements in the clinical setting.

5.2 RECOMMENDATIONS

From the conclusion of this study the following recommendations are addressed to key stakeholders to help achieve higher accuracy in treatment delivery of cancer patients using multi-leaf collimator.

5.2.1 Hospital Management

To the Hospital Management, the following recommendations are made;

- There is a need to adopt this technology of manual multileaf collimator.
- The technology of cutting the leaves into desired shapes should be put in place. With this technology, the tongue and groove design of the leaves can be done in order to produce more leaves. With this initiation in place, lighter weight of leaves will be produced. Moreover, the leaves can be advanced from manual to motorize to improve quality of treatment.

5.2.2Research Community

- Further measurements and improved design should be done to improve the treatment delivery.
- Output factor measurements devices should be made using different water equivalent materials for comparative studies.

REFERENCES

Amand O., Garduno G., Celis M. A., Manuel J., Radiation transmission, leakage and beam penumbra measurements of a micro- multileaf collimator using Gafchromic EBT film, J ApplClin Med Phys, Jun 23:9 (3): 2802,2008.

American Association of Physics in Medicine Report No. 63, Recommendations of AAPM Radiation Therapy Committee Task Group No. 55, Medical Physics, Vol. 25, Issue 11, November, 1998.

American Association of Physics in Medicine Report No. 72, Task Group No. 50, 2006.

Arthur B., Biggs P., Galvin J., Klein E., LoSasso T., Low D., Nah K., Yu C., Applications of multileaf collimators. AAPM Report No.72. Report of Task Group No.50, 2001, Radiation Therapy Committee.

Baumann M., Echner G., Runz A., Schwandtner R., Kurzeja J., Admietz I., Ueltzhoffer S., Schlegel W., A manual multileaf collimator for use in cobalt-60 teletherapy,Deutsches Krebsforschungszentum In Der Helmholtz-Gemeinschaft (dkfz), 2012.

Dumitru M, Rebega L., Praisler M., Strunga E., Dumitrache M., Issue in radiotherapy practice due the presence of wedge filters, Romanian Reports in Physics, Vol.65, No.2, p. 456-467, 2013.

Ferachi K.K., Multileaf collimator reproducibility evaluated with a two –dimensional diode array, Thesis, Department of Physics and Astronomy, Lousiana State University, 2003.

Fischer M., Todrovic M., Drud E., Cremers F., Commissioning of a double-focused micromultileaf, Journal of Applied Clinical Medical Physics, Volume 11, Number 2, Spring 2010.

Gadza M. J., Coia L.R., Principles of radiation therapy, Oncol.Biol.Phys; 60(1): 365-274, 2004.

Galvin J. M.,The multileaf collimator. A complete Guide,Int.J.Rad.Oncol.Biol.Phys. 27:697-705, 1993.

Goadrich L. D., A metaheuristic for IMRT intensity map segmentation, University of Wisconsin-Madison, 2004.

Hariri S, Shariari M., Monte Carlo based suggestion of the best choice for material of a multileaf collimator and the required thickness, World congress on Medical Physics and Biomedical Engineering, Volume 25/1 of the series IFMBE proceedings pp 679-682, 2009.

Hariri S., Shahriari M., Suggesting a new design for multileaf collimator leaves based on Monte Carlo simulation of two commercial systems, J Appl.Clin Med Phys Jun 15;11(3): 3101, 2010.

International Atomic Energy Agency Technical Document (IAEA TECDOC)-1588, 2008.

International Commission of Radiological Protection Publication 103, 2007.

Jaffray D. A., Battista J.J., Fenster A., Munro P, X-ray sources of medical linear accelerators : focal and extra-focal radiation, Med Phys. 20 (5): 1417-27; 1993.

Jeraj M., Robar V., Multileaf collimator in Radiotherapy, Radiol. Oncol; 38(30): 235-40, 2004.

Khan F. M., The physics of radiation therapy, 3rd Edition, ISBN 0-7817-3065-1 chapter 13, 2003.

Kotb O., Elsahat M. O., Eldebawi N. M., Nasif A, Mansour E., Dosimetric evaluation of the MLCs for irregular shaped radiation fields, IOSR Journal of Applied Physics (ISOR-JAP) e-ISSN:2278-4861. Volume 5, Issue 3, pp 57-63, Nov.-Dec. 2013.

LoSasso T., Shou C., Ling C.C., Physical and dosimetric aspects of a multileaf collimation system used in the dynamic mode for implementing intensity modulated radiotherapy, Med Phys, 25(10):1919-27, 1998.

Luxton G., Joszef G., Astrahan M.A., Algorithm for dosimetry of multiarc linear accelerator stereotactic radiosurgery; Med Phys. 18(6):1211–21. 1991.

Parker W., Patrocinio H., Clinical treatment planning in external photon beam radiotherapy, Review of radiation oncology physics: A handbook for teachers and students, IAEA publication (ISBN 92-0-107304-6), 2005.

Power, W.E., Kinzie J.J., Demidecki J.A., Bradfield J.S., Feldman A., A new system of field shaping for external-beam radiation therapy Radiol.108: 407-411,1973.

Sharma S.C., Beam modification devices, Department of Radiotherapy, Postgraduate Institute of Medical Education and Research, 2012.

Topolnjak R., The six-bank multi-leaf system, A large field size, high resolution collimator for advanced radiotherapy, Phy. Med. Biol, 50(9): 2015-31, 2005.

Toossi M.T., Hashemian A., Nassesi S., Design and fabrication of the control part of a prototype multileaf collimator; J Med Sig.Sens. pp 300-304, 2014.

Williams J.I., Thwaites D.I., Radiotherapy physics in practice, ISBN 0-19-262878-x, 1993.

Wong V.Y.W., Quality assurance devices for dynamic conformal radiotherapy, Journal of Applied Clinical Medical Physics, Vol 5, No 1,2004.

www.medicalphysics.org, 12/01/2015.

www.ncbi.com 12/10/2015

Xing L, Thorndyke B, Schreibmann E, Yang Y, Li Tf, Kim Gy, Luxton G, Koong A, Overview of image-guided radiation therapy, Med Dosim. 31(2): 91-112, 2006.

APPENDIX

APPENDIX-I

Leakage measurements for Co-60teletherapy unit using a chamber calibrated in terms of N_{DW} practical data.

No.	Reading [pC]	Time: t [s]	Reading Rate [nC $250s^{-1}$]
1	- 1.71	60	-0.4275
2	- 1.77	60	-0.4425
3	- 1.77	60	-0.4425
4	- 1.77	60	-0.4425
5	- 1.78	60	-0.445
Mean	-1.76	60	-0.440

APPENDIX- II

Collimator Scatter Factor for square fields of a Cirus Cobalt-60 teletherapy treatment machine practical data.

Field Size	Reading [nC] for 60 seconds (1 minute)				
	1	2	3	4	Mean Q_{mean}
10 x 10	2.739	2.737	2.741	2.745	2.7405
4 x 4	2.343	2.346	2.347	2.348	2.346
5 x 5	2.413	2.415	2.418	2.415	2.415
6 x 6	2.538	2.539	2.540	2.541	2.540
7 x 7	2.607	2.607	2.608	2.608	2.607

8 x 8	2.704	2.706	2.705	2.706	2.705
9 x 9	2.749	2.749	2.749	2.750	2.749
10 x 10	2.843	2.842	2.843	2.844	2.843
12 x 12	2.958	2.958	2.959	2.960	2.958
15 x 15	3.165	3.166	3.168	3.172	3.167
20 x 20	3.519	3.520	3.521	3.521	3.520
25 x 25	3.792	3.792	3.793	3.794	3.793
30 x 30	4.038	4.038	4.038	4.038	4.038
32 x 32	4.103	4.103	4.102	4.104	4.103
Std. dev.	$\left(\frac{Max\ Value - mean}{mean}\right) = 0.00118$				

APPENDIX – III.a.Output factors for open MLC field data

Square field size (cm)	**Relative Output (nC) for various depths**			
4 x 4	0.00097	0.014	0.044	0.072
10 x 10	1	1	1	1
15 x 15	1.155	1.098	1.135	1.164
20 x20	1.195	1.159	1.227	1.275
26 x 26	1.229	1.206	1.291	1.362
32 x 32	1.258	1.237	1.329	1.406

APPENDIX – III.b. Output factors for closed MLC field data

Square field size (cm)	Relative Output (nC) for various depths			
	0.5	5	10	15
4 x 4	0.041	0.046	0.058	0.092
10 x 10	1	1	1	1
15 x 15	1.145	1.184	1.228	1.277
20 x20	1.30	1.351	1.409	1.491
26 x 26	1.475	1.535	1.610	1.728
32 x 32	1.630	1.724	1.783	1.913

APPENDIX- IV.a. MLC effect for 15 cm x 15 cm field size data

Field size (cm)	Output factors (nC)			
	0.5	5	10	15
7.5 x 7.5	0.309	0.283	0.309	0.263
10 x 10	1	1	1	1
15 x 15	1.306	1.210	1.183	1.245
20 x 20	1.424	1.259	1.238	1.335
23 x 15	1.466	1.272	1.271	1.349
23 x 20	1.514	1.287	1.267	1.386
26 x 23	1.592	1.309	1.291	1.432
26 x 26	1.645	1.321	1.299	1.447
32 x 32	1.759	1.349	1.340	1.507

APPENDIX- IV.b. MLC effect for 7.5 cm x 7.5 cm field size data

Field size (cm)	Output factors (nC)			
	0.5	5	10	15
7.5 x 7.5	0.263	0.283	0.450	0.543
10 x 10	1	1	1	1
15 x 15	1.245	1.210	1.141	1.146
20 x 20	1.335	1.259	1.199	1.217
23 x 15	1.349	1.272	1.211	1.229
23 x 20	1.386	1.287	1.229	1.246
26 x 23	1.432	1.309	1.252	1.270
26 x 26	1.447	1.447	1.262	1.281
32 x 32	1.507	1.349	1.293	1.308

APPENDIX-V Transmission factor raw data.

Field sizes for open fields	closed fields
32 x32	32x32
0.082	0.016
1.139	0.173
1.326	0.221
1.452	0.258
1.552	0.299
1.602	0.331